Coordination Chemistry Reviews 255 (2011) 161–185

Contents lists available at ScienceDirect

Coordination Chemistry Reviews

journal homepage: www.elsevier.com/locate/ccr

Review

Bis(oxalato)chromium(III) complexes: Versatile tectons in designing heterometallic coordination compounds

Gabriela Marinescu[a,b], Marius Andruh[b,*], Francesc Lloret[c], Miguel Julve[c,*]

[a] Institute of Physical Chemistry of the Romanian Academy, Coordination Chemistry Laboratory, Spl. Independentei nr. 202, 060021 Bucharest, Romania
[b] Inorganic Chemistry Laboratory, Faculty of Chemistry, University of Bucharest, Str. Dumbrava Rosie nr. 23, 020464 Bucharest, Romania
[c] Departament de Química Inorgànica/Instituto de Ciencia Molecular (ICMol), C/Catedrático José Beltrán no. 2, 46980 Paterna (Valencia), Spain

Contents

ARTICLE INFO

Article history:
Received 23 June 2010
Received in revised form 2 August 2010
Accepted 8 August 2010
Available online 17 August 2010

Dedicated to Professor Herbert W. Roesky, on the occasion of his 75th birthday, as a tribute for his spectacular achievements in the field of inorganic chemistry.

Keywords:
Chromium(III) complexes
Oxalato complexes
Heterometallic complexes
Magnetic properties

ABSTRACT

The mononuclear oxalato-containing chromium(III) complexes of general formula $[Cr(AA)(C_2O_4)_2]^-$ (AA = α-diimine type ligand) are able to produce a large variety of heterometallic complexes by acting as ligands towards either fully solvated metal ions or preformed cationic complexes with available coordination sites. This review focuses on the structural diversity of the polynuclear complexes (oligonuclear and coordination polymers) which are generated by the bis(oxalato)chromate(III) species, with a special emphasis to their magnetic properties.

Abbreviations: $H_2C_2O_4$, oxalic acid; Hacac, acetylacetone; bipy, 2,2′-bipyridine; Hbpca, bis(2-pyridylcarbonyl)amide; dmbipy, 4,4′-dimethyl-2,2′-bipyridine; 4,4′-bipy, 4,4′-bipyridine; bpym, 2,2′-bipyrimidine; dpa, dipyridylamine; phen, 1,10-phenanthroline; H_2salen, *N*,*N*′-ethylenebis(salicylideneimine); PPh_4^+, tetraphenylphosphonium; $AsPh_4^+$, tetraphenylarsonium; NBu_4^+, tetra-*n*-butylammonium; 4-NH_3-py$^+$, 4-aminopyridinium; MeOH, methanol; MeCN, acetonitrile; dmf, dimethylformamide; hm, histamine; BEDT-TTF, bis(ethylenedithio)tetrathiafulvalene; bpp, 2,6-bis(pyrazol-3-yl)pyridine; dpno, 4,4′-bipyridine-*N*,*N*′-dioxide; H_2valen, *N*,*N*′-ethylenebis(3-methoxysalicylideneimine); H_2fsaaep, 3-[*N*-2-(pyridylethyl)formimidoyl]salicylic acid; 6,6′-dmbipy, 6,6′-dimethyl-2,2′-bipyridine; H_2L^1, bicompartmental Schiff-base resulting from the stepwise condensation of 2,6-diformyl-*p*-cresol with ethylenediamine and diethylenetriamine; H_2L^2, *N*,*N*′-propylenebis(3-methoxysalicylideneimine); pyim, 2-(2′-pyridyl)imidazole; bpm, bis(1-pyrazolyl)methane; en, ethylenediamine.

* Corresponding authors.
E-mail addresses: marius.andruh@dnt.ro (M. Andruh), Miguel.Julve@uv.es (M. Julve).

0010-8545/$ – see front matter © 2010 Elsevier B.V. All rights reserved.
doi:10.1016/j.ccr.2010.08.004

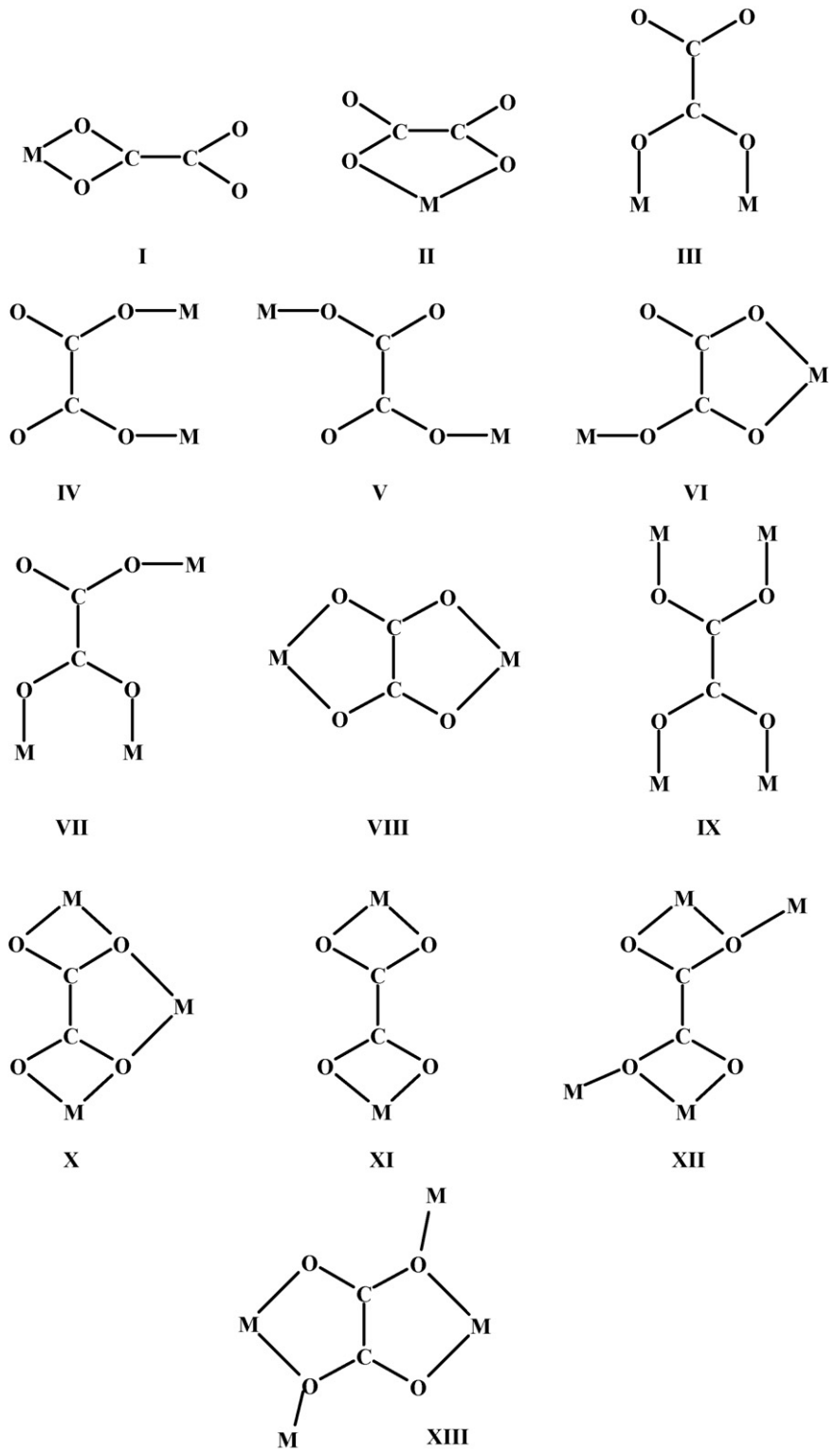

Scheme 1.

1. Introduction

The chemistry of multimetallic complexes is nowadays a broad and interdisciplinary research field. Crystal engineering, molecular magnetism, catalysis, biomimetic coordination chemistry are only few hot topics asking for new synthetic routes leading to homo- or heteropolynuclear complexes with pre-established structures, properties and functions.

The ability of the oxalate anion to generate homo- and heteropolynuclear complexes is well known. The rich structural diversity of the oxalato-bridged complexes (ranging from binuclear species to high-nuclearity compounds and to coordination polymers with various dimensionalities and network topologies) is due to the exceptional versatility of the oxalato ligand (Scheme 1). Moreover, the oxalato bridge can efficiently mediate the exchange interactions between the paramag-

netic metal ions, leading to interesting magnetic properties [1].

A great number of oxalato-bridged homopolynuclear complexes have been characterized so far. These compounds are generally obtained through the reaction between a cationic complex having potentially free coordination sites and the oxalate anion. The presence of an ancillary organic ligand within the coordination sphere of the metal ion prevents the formation of highly insoluble chain compounds of general formula $M(C_2O_4)\cdot nH_2O$ (M being a divalent metal ion and $C_2O_4^{2-}$ the dianion of the oxalic acid). As far as the heterometallic complexes are concerned, their synthesis raises an important point: the one-pot procedure (the reaction of two different metal ions with the oxalate anion) leads to mixtures of compounds and then it has to be discarded. In order to overcome this difficulty, an alternative synthetic strategy has been developed. It consists of using anionic oxalato-containing mononuclear complexes (metalloligands or building blocks) as ligands towards the second metal ion. This synthetic route, which is referred to as the "complex as ligand strategy", is actually a self-assembly process involving anionic tectons and assembling cations.

Considering the heteropolynuclear oxalato complexes, the very first attempts provided a heterobimetallic oxalato-bridged Cu(II)Ni(II) chain using the bis(oxalato)cuprate(II) anion ($[Cu(C_2O_4)_2]^{2-}$) as a building block [2]. However, this precursor is very labile. In fact, its easy loss of one oxalato ligand, which is accompanied by the precipitation of the copper(II) chain $CuC_2O_4\cdot 1/3H_2O$, makes this precursor unsuitable for synthetic purposes in solution. It is clear that very stable species as metalloligands are required, such as six-coordinated complexes of chromium(III), low-spin iron(III) or low-spin cobalt(III), which are characterized by a high CFSE and inert character regarding the ligand dissociation. Homo- and heteroleptic anionic complexes of chromium(III) with one or more potentially bridging oxalato groups such as $[Cr(salen)(C_2O_4)]^-$, $[Cr(acac)_2(C_2O_4)]^-$ and $[Cr(C_2O_4)_3]^{3-}$ are particularly useful for the design of heterometallic oxalato-bridged systems of interest in molecular magnetism. They are relatively stable species towards substitution reactions and *a priori* they can ensure a good control over the reaction products. The two first ones would generate heterobinuclear complexes when the second metal ion has one or two available coordination sites, the others being blocked by an auxiliary ligand [3]. The last one, with three potentially bridging ligands, is more appropriate for the synthesis of high-dimensionality coordination polymers, as evidenced by the extremely rich chemistry which has been developed based upon this tris(oxalato)chromate(III) anion [4]. In fact, a large variety of heterometallic oxalato-bridged complexes have been obtained through self-assembly processes involving the chromium(III) building block, $[Cr(C_2O_4)_3]^{3-}$, and either fully solvated transition metal ions, or cationic complexes whose coordination sphere is unsaturated (assembling cations). It has been shown that for complexes with the general formula $cat[MCr(C_2O_4)_3]$ the countercations, cat^{n+}, play a crucial role in stabilizing the 2- or 3D networks. Honeycomb structures of formula $XR_4[M(II)Cr(C_2O_4)_3]$ were obtained when the cation is of the type XR_4^+ (X = N or P; R = alkyl or aryl) or even the decamethylmetallocenium unit [5]. Their structure consists of an anionic sublattice, $[MCr(C_2O_4)_3]^{n-}{}_n$ and the cationic counterpart. The two metal ions, M(II) and Cr(III), are connected by bis-bidentate oxalate groups. It is important to recall here that the $[M(C_2O_4)_3]^{3-}$ species exhibits a propeller-like chirality (Δ and Λ). Within the heterometallic network both metal centers are chiral. If the absolute configurations of the connected centers are different, [Δ(M)/Λ(Cr)] or [Λ(M)/Δ(Cr)], then the resultant coordination polymers are two-dimensional with a honeycomb topology. 2D optically active Mn^{II}–Cr^{III} polymers can be obtained [i.e. crystals containing only one type of bimetallic layer [(Δ – Cr^{III}/Λ – Mn^{II}) or (Λ – Cr^{III}/Δ – Mn^{II})] in the cases where only one enantiomeric form is used (Δ – $[Cr(C_2O_4)_3]^{3-}$ or Λ – $[Cr(C_2O_4)_3]^{3-}$) or using the chiral templating activity of a resolved precipitating cation [5g,j,k,l]. Some of these systems are examples of multifunctional molecular materials because in addition to their interesting magnetic properties, they exhibit predesigned chirality [4h,5g,j,k,l], electrical conductivity [5i], magneto-chiral dichroism [5l], spin crossover [6], nonlinear optics activity [7] and proton conduction [8]. Chiral anionic 3D networks of formula $[M^{II}_2(C_2O_4)_3]^{2n-}{}_n$, $[M^{I}M^{III}(C_2O_4)_3]^{2n-}{}_n$ and $[M^{II}M^{III}(C_2O_4)_3]^{n-}{}_n$ were obtained when using the tris-chelated $[M(bipy)_3]^{2+/3+}$ (bipy = 2,2′-bipyridine) as templated cation [5g,9]. Recently, two more uncommon homoleptic oxalato complexes ($[M^{IV}(C_2O_4)_4]^{4-}$ with M = Zr and U) were used as building blocks to construct diamondoid 3D coordination polymers [10].

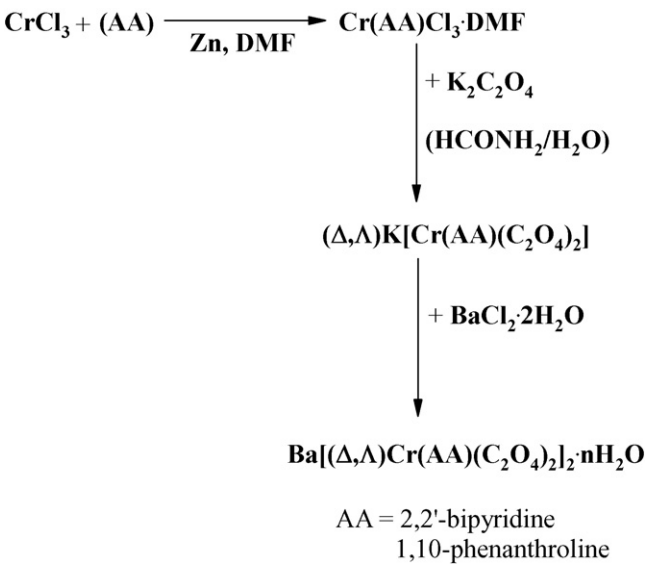

Scheme 2.

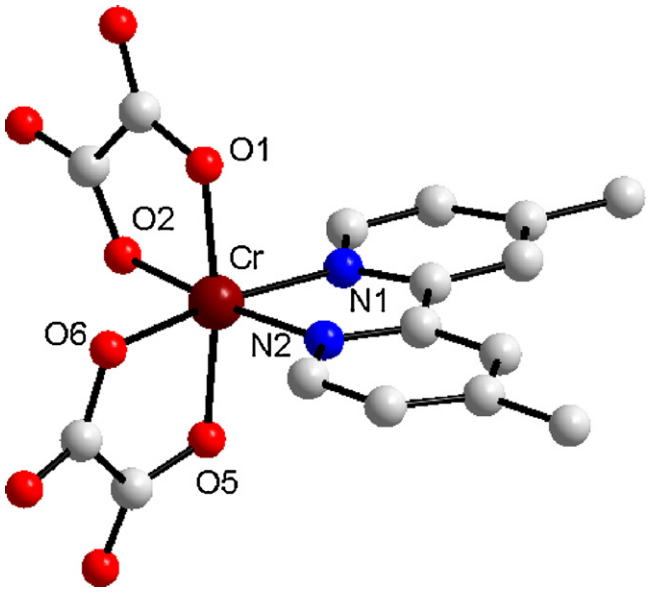

Fig. 1. Perspective view of the mononuclear anion in $AsPh_4[Cr(dmbipy)(C_2O_4)_2]\cdot 5H2O$ **5b**. Color code: carbon, grey; oxygen, red; nitrogen, blue; chromium, purple.
Adapted from Ref. [17].

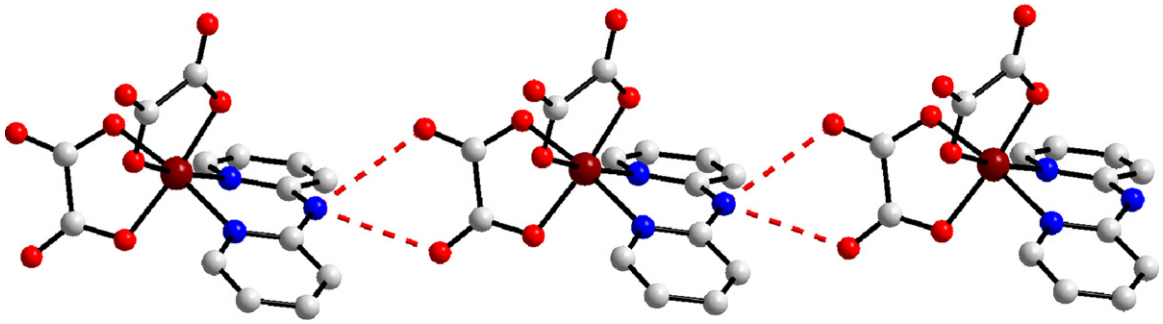

Fig. 2. Hydrogen-bonded chain of $[Cr(dpa)(C_2O_4)_2]^-$ units in **3a**.
Adapted from Ref. [15].

The library of oxalato complexes to be used as tectons in designing supramolecular solid-state architectures was enriched by heteroleptic anionic complexes $[Cr(AA)(C_2O_4)_2]^-$ [AA = 2,2′-bipyridine (bipy), 4,4′-dimethyl-2,2′-bipyridine (dmbipy), 1,10-phenanthroline (phen), 2,2′-dipyridylamine (dpa) and 2,2′-bipyrimidine (bpym)], which are obtained by replacing one oxalato group within the tris(oxalato)chromate(III) anion by a neutral bidentate ligand, AA. This paper reviews the chemistry generated by these anionic complexes through their use as ligands focusing on the diversity of the structures of the resulting heterobimetallic species as well as on their magnetic properties.

2. General synthetic procedures

The first step in the preparative route of the oxalato-bridged heterobimetallic complexes consists of synthesizing the heteroleptic mononuclear precursors, $[Cr(AA)(C_2O_4)_2]^-$. The bipy and phen derivatives ($[Cr(bipy)(C_2O_4)_2]^-$ and $[Cr(phen)(C_2O_4)_2]^-$) were synthesized by Broomhead in the early '60s, starting from anhydrous $CrCl_3$, as illustrated in Scheme 2 [11]. The corresponding barium(II) salts, $Ba[Cr(bipy)(C_2O_4)_2]_2{\cdot}nH_2O$ and $Ba[Cr(phen)(C_2O_4)_2]_2{\cdot}nH_2O$, which are themselves interesting coordination polymers (see Section 5) can be used directly in synthesizing heterobimetallic complexes, by reacting them with the appropriate metal sulfate, taking advantage of the insolubility of the barium sulfate.

An alternative synthetic procedure for the bis-oxalato chromium(III) complexes is the one-pot reaction between $CrCl_3{\cdot}6H_2O$, the organic chelating ligand (AA), and sodium oxalate under reflux [Cr(III)/AA/$C_2O_4^{2-}$ in a 1:1:2 molar ratio]. The subsequent addition of an organic cation affords crystalline complexes of formula $XPh_4[Cr(AA)(C_2O_4)_2]$ (X = P or As) [12–15]. In comparison with the sodium or potassium derivatives, which are soluble in water, the $XPh_4[Cr(AA)(C_2O_4)_2]$ complexes show a good solubility in common organic solvents (MeOH or MeCN, for instance).

New heterometallic complexes can be obtained by following one of the routes mentioned hereunder:

(a) Transmetallation reactions using the barium precursors and the desired metal ion as a sulfate salt; the insoluble barium sulfate is removed by filtration, and the solution is allowed to evaporate to favour the crystallization of the corresponding oxalato-bridged heterometallic complex.
(b) Transmetallation reactions between the water-soluble sodium or potassium precursors and the metal salts.
(c) Methathesis reactions involving the $XPh_4[Cr(AA)(C_2O_4)_2]$ precursors and the desired metal ions as perchlorate salts.

In all these cases, the assembling cation is coordinated solely by the solvent molecules, or, eventually, by the accompanying anion. The self-assembly process can also occur in the presence of ancil-

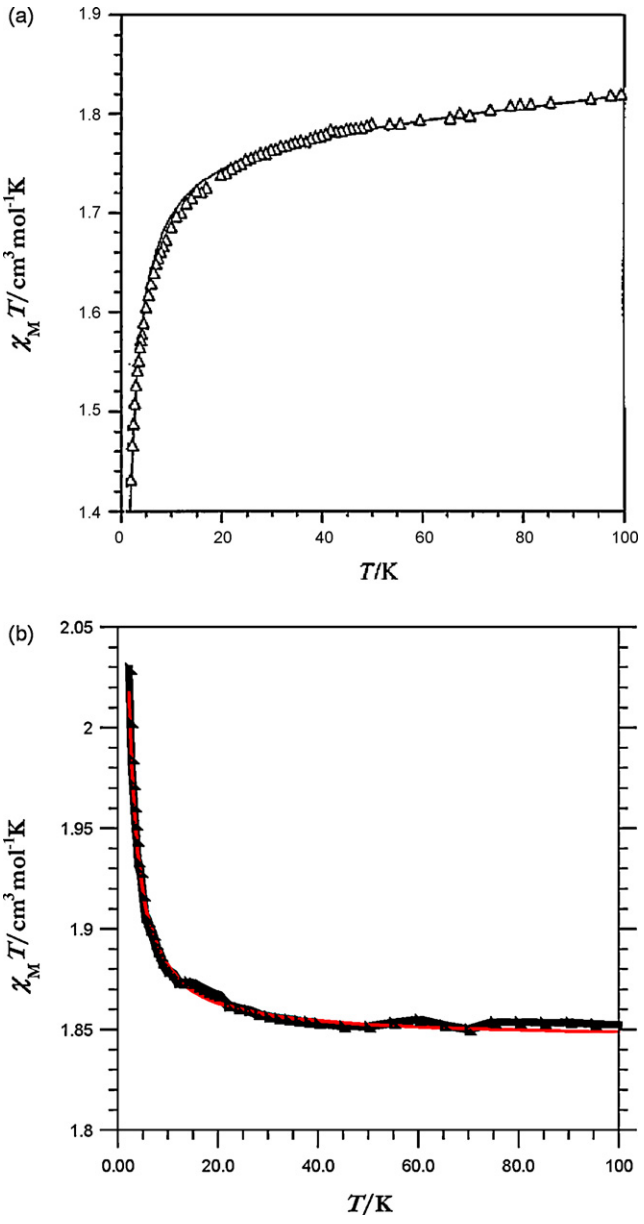

Fig. 3. $\chi_M T$ versus T plots for compounds **1a** (a) and **5b** (b).
Adapted from Refs. [12,17].

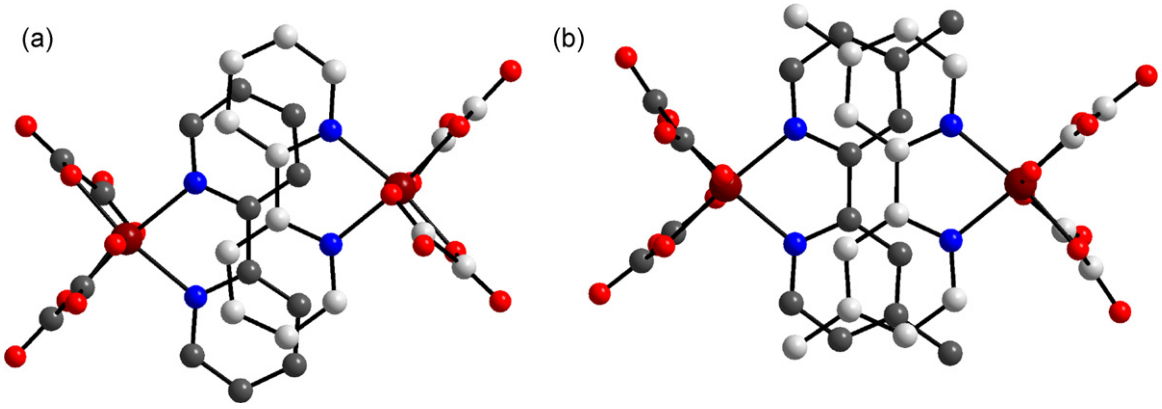

Fig. 4. Crystal packing of the $[Cr(AA)(C_2O_4)_2]^-$ entities in **1a** (a) and **5b** (b).
Adapted from Refs. [12,17].

lary ligands that coordinate to the assembling cation. Their role is to block some coordination sites at the assembling cation and consequently, to influence the architecture of the resulting polynuclear complex. The $[Cr(AA)(C_2O_4)_2]^-$ tectons are chiral, and the participation of one or of both enantiomers in the building process has also structural consequences.

Although the $[Cr(AA)(C_2O_4)_2]^-$ mononuclear precursors are quite robust species and their integrity is normally preserved in their complexation reactions, a partial decomposition in solution has been observed for some cases where the release of the neutral bidentate AA ligand or the oxalate groups occurred (see below).

3. Mononuclear complexes

The crystal structures of several mononuclear complexes of interest for this paper have been solved: $AsPh_4[Cr(bipy)(C_2O_4)_2]\cdot H_2O$ **1a** [12], $PPh_4[Cr(bipy)(C_2O_4)_2]\cdot H_2O$ **1b** [13], $AsPh_4[Cr(phen)(C_2O_4)_2]\cdot H_2O$ **2** [14], $PPh_4[Cr(dpa)(C_2O_4)_2]$ **3a**, $AsPh_4[Cr(dpa)(C_2O_4)_2]$ **3b**, [15] $PPh_4[Cr(bpym)(C_2O_4)_2]\cdot H_2O$ **4** [16], $PPh_4[Cr(dmbipy)(C_2O_4)_2]\cdot 5H_2O$ **5a** and $AsPh_4[Cr(dmbipy)(C_2O_4)_2]\cdot 5H_2O$ **5b** [17]. Fig. 1 shows the molecular structure of one of them, namely the anionic complex in **5b**. The cations are innocent, so they do not bind to the oxalato groups, which act only as terminal ligands towards the chromium(III) ion. Separate stacking of the anions and cations is observed in the crystal structures and, in the case where the AA ligand has the possibility of acting as a hydrogen donor, the complex anions are hydrogen bonded (case of dpa in **3a** where $N–H_{dpa}\cdots O_{ox}$ hydrogen bonds are present as shown in Fig. 2). The crystal structures of the mononuclear anionic species, $[Cr(AA)(C_2O_4)_2]^-$, are useful in analyzing the interatomic distance within the oxalato groups while acting as bridges, in comparison with the bond distances associated to the terminal oxalato ligands. For the terminal oxalato groups, two sets of carbon–oxygen bond distances are observed, the shortest values belonging to the peripheral C–O bonds, in agreement with their greater double bond character. The ranges of values for the outer and inner C–O bonds for the particular case of **5b** are 1.215(4)–1.226(4) and 1.263(4)–1.291(4) Å, respectively. The chromium(III) ion is coordinated by two nitrogen atoms arising from the organic ligand and four oxygen atoms, adopting a distorted octahedral geometry. The short values for the bites of the chelating α-diimines and oxalato ligands are the main factors responsible for the distortion from the ideal octahedral geometry.

Several similar phenanthroline-containing derivatives have been reported: $4\text{-}NH_3\text{-}Py[Cr(phen)(C_2O_4)_2]\cdot 2H_2O$, $NBu_4[Cr(phen)(C_2O_4)_2]$ and $PPh_4[Cr(phen)(C_2O_4)_2]$ [18]. We mention also that $[Cr(AA)(C_2O_4)_2]^-$ mononuclear complexes have been used as counterions in molecular materials exhibiting

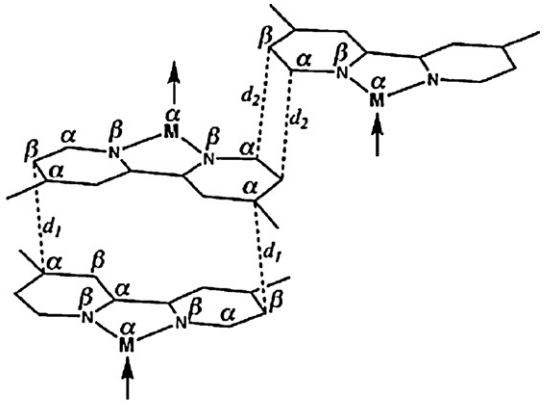

$d_1 = 3.39$ Å; $d_2 = 3.27$ Å

Scheme 3.

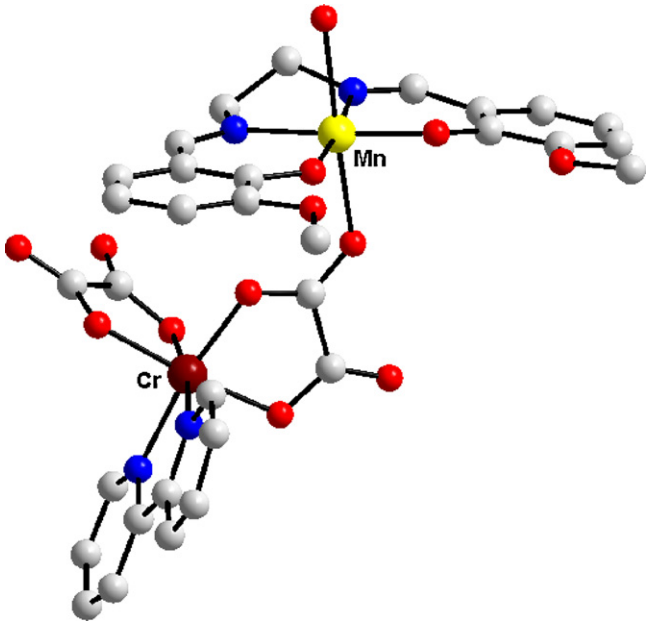

Fig. 5. Perspective view of the neutral heterobimetallic dinuclear complex $[\{Mn(H_2O)(valen)\}\{Cr(bipy)(C_2O_4)_2\}]\cdot 3H_2O$ **6a**.
Adapted from Ref. [24].

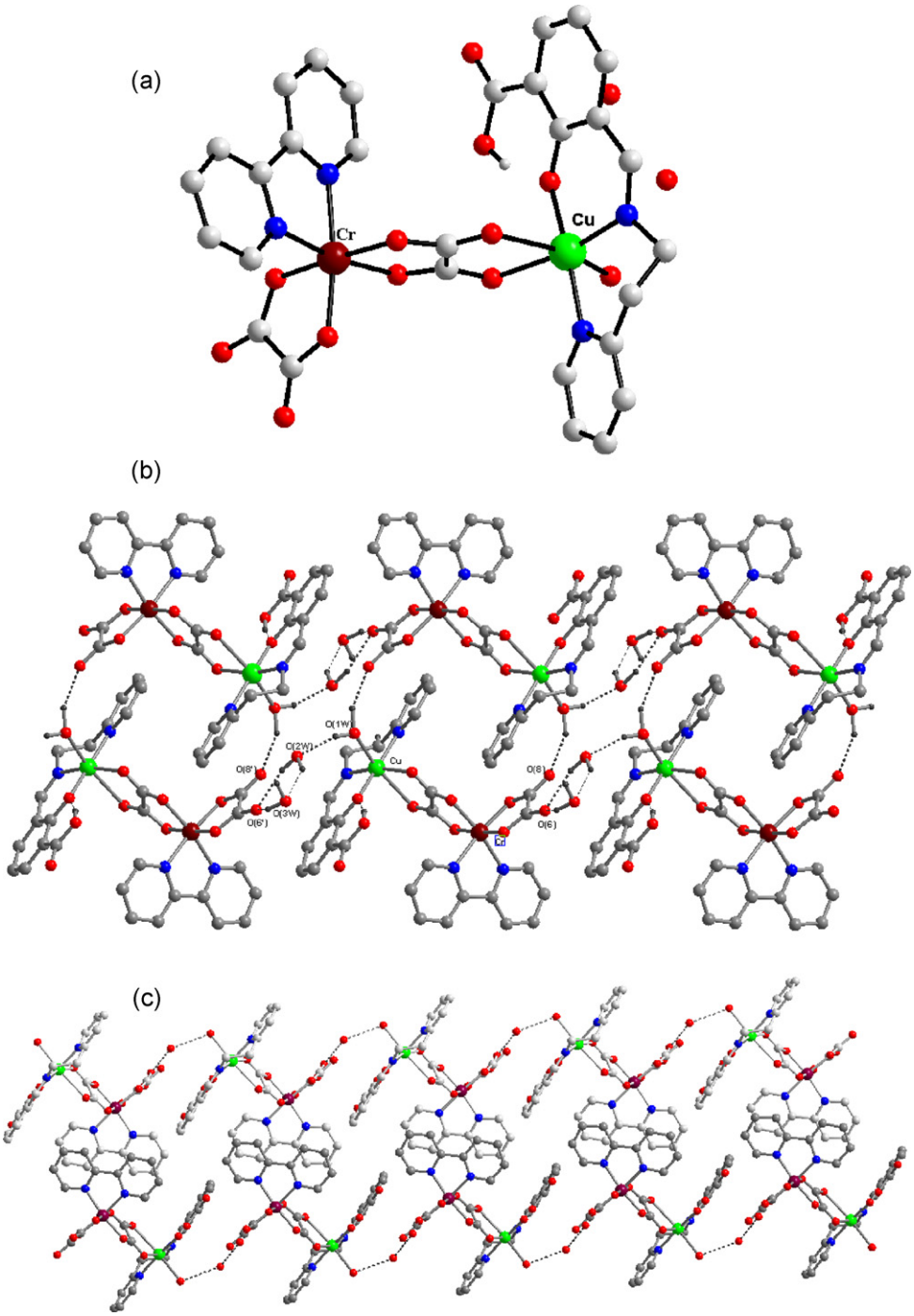

Fig. 6. (a) Crystal structure of the heterobimetallic dinuclear complex [{Cu(Hfsaaep)}{(Cr(bipy)(C_2O_4)$_2$}]·2H_2O **7**; (b) supramolecular chain resulted from hydrogen bond interactions between the binuclear [CuCr] units and the water molecules; and (c) detail of the packing diagram showing the π–π stacking interactions between the bipy ligands.
Adapted from Ref. [25].

electric conductivity, (BEDT-TTF)$_2$[Cr(bipy)(C_2O_4)$_2$]·$CHCl_2CH_2Cl$ [BEDT-TTF = bis(ethylenedithio)tetrathiafulvalene] [19], or spin crossover, [Fe(bpp)$_2$][Cr(AA)(C_2O_4)$_2$]·$n$$H_2O$ [bpp = 2,6-bis(pyrazol-3-yl)pyridine; AA = bipy and phen] [20].

The interesting supramolecular motifs occurring through π–π contacts in crystals containing complexes with the general formula PPh_4[M(phen)(C_2O_4)$_2$] (M = Co and Cr) were analyzed by Dance et al. [21]. One of the goals of their research is to identify the different embrace domains between the hydrophobic components, to further design and engineer the structures of the molecular crystals with analogous metal complex units.

The magnetic properties of the mononuclear complexes **1**–**5** were investigated as a function of the temperature [12–17]. Two factors are responsible for their magnetic behaviour: (i) the zero field splitting (D) of the ground state of Cr(III), which is described be the Hamiltonain: $\boldsymbol{H} = D[\boldsymbol{S}_z{}^2\text{-}(1/3)S(S+1)]$; (ii) the exchange interactions at the supramolecular level (θ), mediated by π–π stacking of the aromatic ligands and, eventually, hydro-

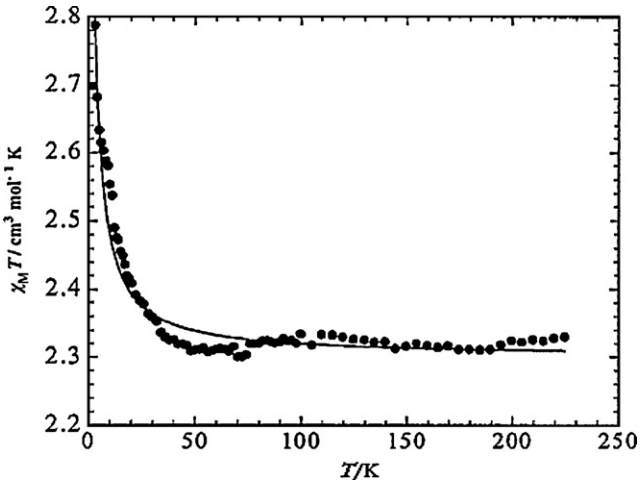

Fig. 7. $\chi_M T$ versus T plot for compund **7**.
Adapted from Ref. [25].

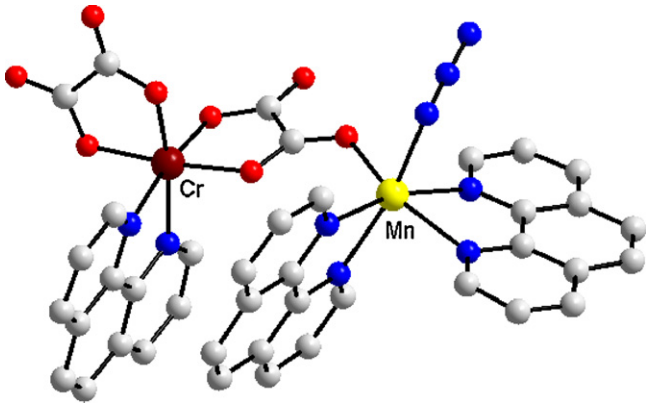

Fig. 9. View of the neutral heterobimetallic complex [{Mn(phen)$_2$(N$_3$)}{Cr(phen)(C$_2$O$_4$)$_2$}]·H$_2$O **9**.
Adapted from Ref. [25].

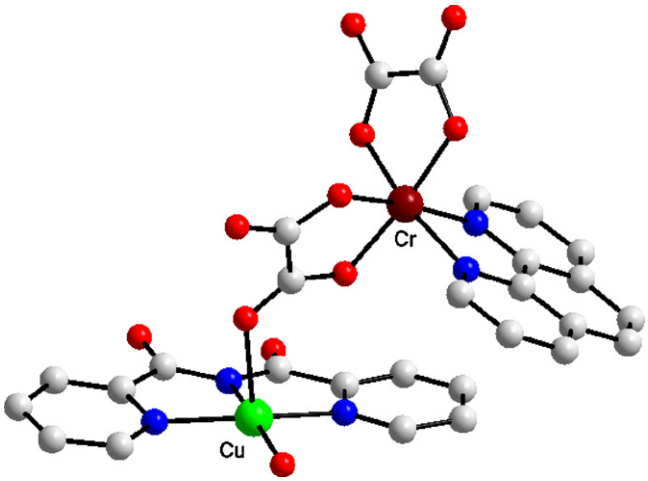

Fig. 8. Crystal structure of [{Cu(bpca)}{Cr(phen)(C$_2$O$_4$)$_2$}]·2H$_2$O **8b**.
Adapted from Ref. [13].

gen bonds involving the oxalato oxygens and crystallization water molecules.

The temperature dependence of the magnetic susceptibility for a mononuclear chromium(III) complex is given by Eqs. (1)–(3).

$$\chi_M = \frac{N\beta^2 g^2}{3k(T-\theta)}(\chi_{II} + 2\chi_{\perp}) \quad (1)$$

with

$$\chi_{II} = \frac{1 + 9\ \exp(-2D/kT)}{4(1+\exp(-2D/kT))} \quad (2)$$

and

$$\chi_{\perp} = \frac{4 + (3kT/D)[1-\exp(-2D/kT)]}{4[1+2\ \exp(-2D/kT)]} \quad (3)$$

where: T = temperature, k = Boltzmann constant, N = Avogadro number, g = Landé factor and β = Bohr magneton.

Let us discuss here the cryomagnetic properties of AsPh$_4$[Cr(bipy)(C$_2$O$_4$)$_2$]•H$_2$O **1a** and AsPh$_4$[Cr(dmbipy)(C$_2$O$_4$)$_2$]•5H$_2$O **5b**. Their magnetic behaviour in the low temperature regime is different: the $\chi_M T$ product decreases by lowering the temperature for the first compound (Fig. 3a), while it increases for the second one (Fig. 3b). These differences can be understood by analyzing the packing of the mononuclear species in the crystal.

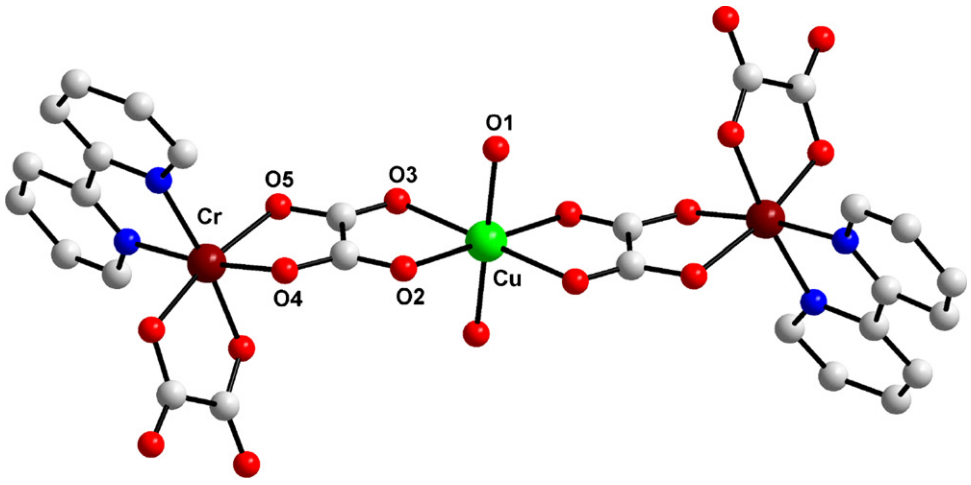

Fig. 10. View of the trinuclear complex [{Cu(H$_2$O)$_2$}{Cr(bipy)(C$_2$O$_4$)$_2$}$_2$]·1.5H$_2$O **12**.
Adapted from Ref. [28].

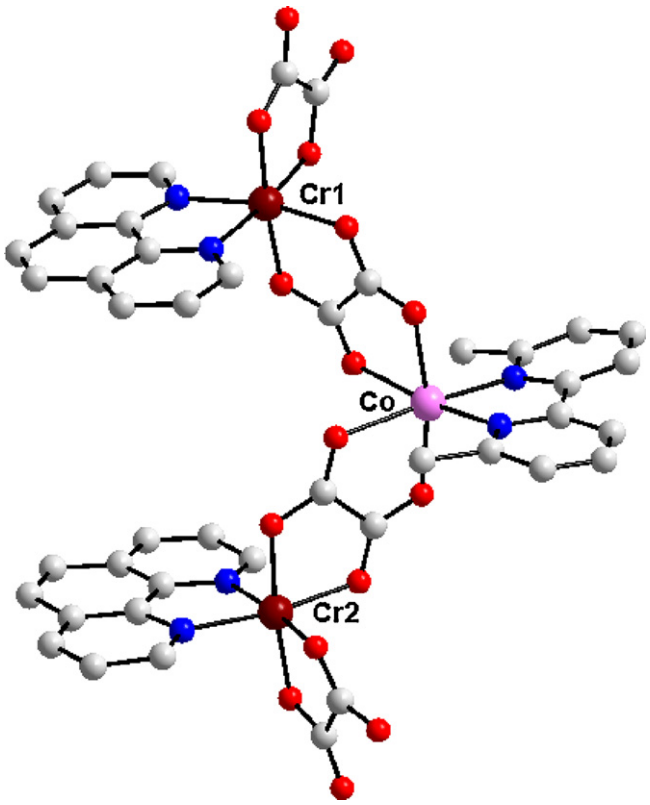

Fig. 11. Perspective view of the trinuclear complex [{Co(6,6′-dmbipy)}{Cr(phen)(C_2O_4)$_2$}$_2$]·1.5H_2O **13b**.
Adapted from Ref. [29].

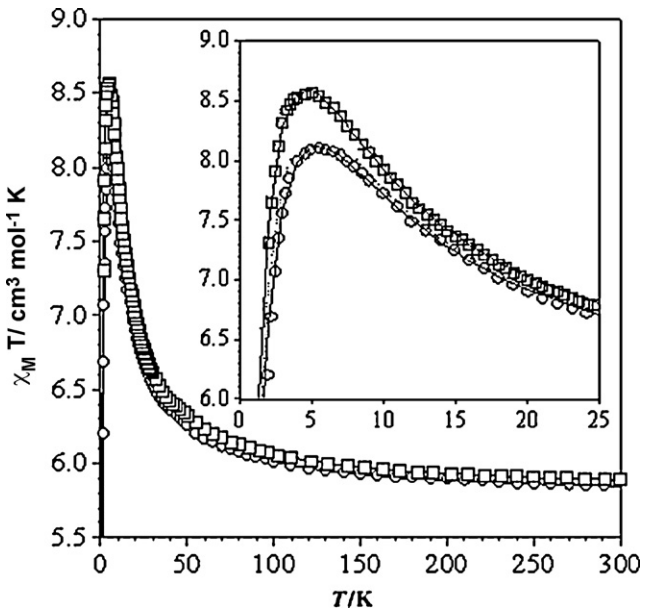

Fig. 12. $\chi_M T$ versus T plots for **13a** (○) and **13b** (□). The inset shows the maxima of $\chi_M T$ in the low temperature region.
Adapted from Ref. [29].

A detail of the packing diagram for **1a** and **5b** is shown in Fig. 4. It is known that magnetic interactions of different nature (either ferro-, antiferromagnetic) can be mediated by the π–π overlap of the organic ligands [22]. Such a different nature of the magnetic coupling can be explained in the frame of the spin-polarization mechanism which was proposed by McConnell [23]. According to this mechanism, molecular units showing uncompensated regions of positive (α) and negative (β) spin densities, arising from spin-polarization effects, are required. If the stacking of the molecules in the crystal is in such a way that the positive spin density of a given unit interacts in an up–down fashion with the negative spin density of the adjacent unit, then the molecular spins are aligned along the same direction, leading to an intermolecular ferromagnetic coupling. This is the case of compound **5b**, as illustrated in Scheme 3. For compound **1a**, the

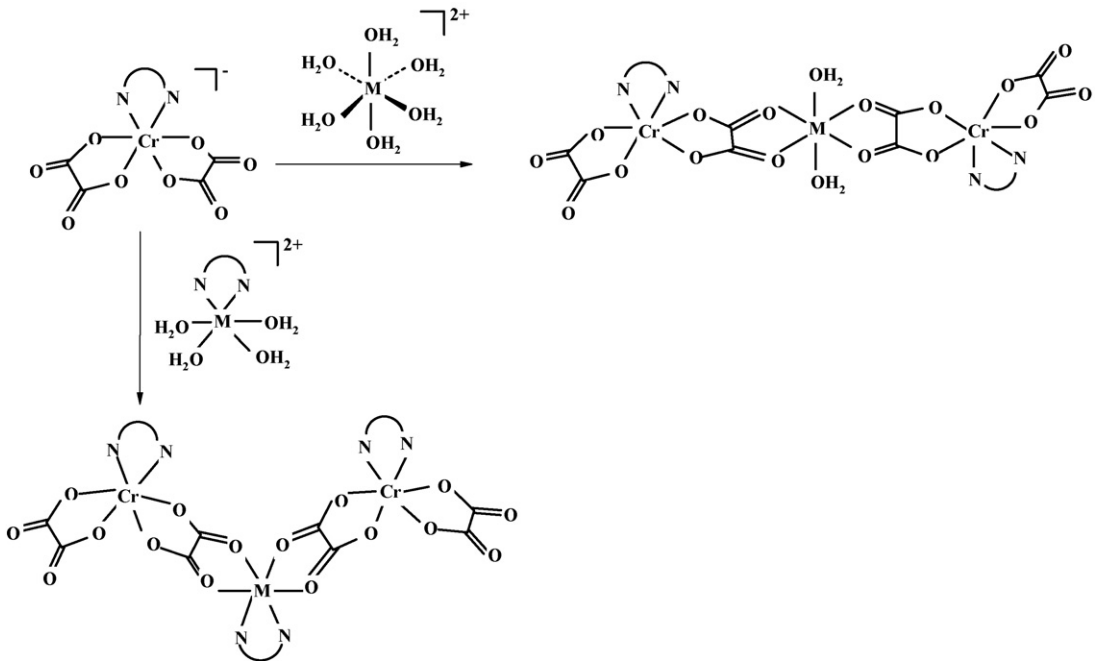

Scheme 4.

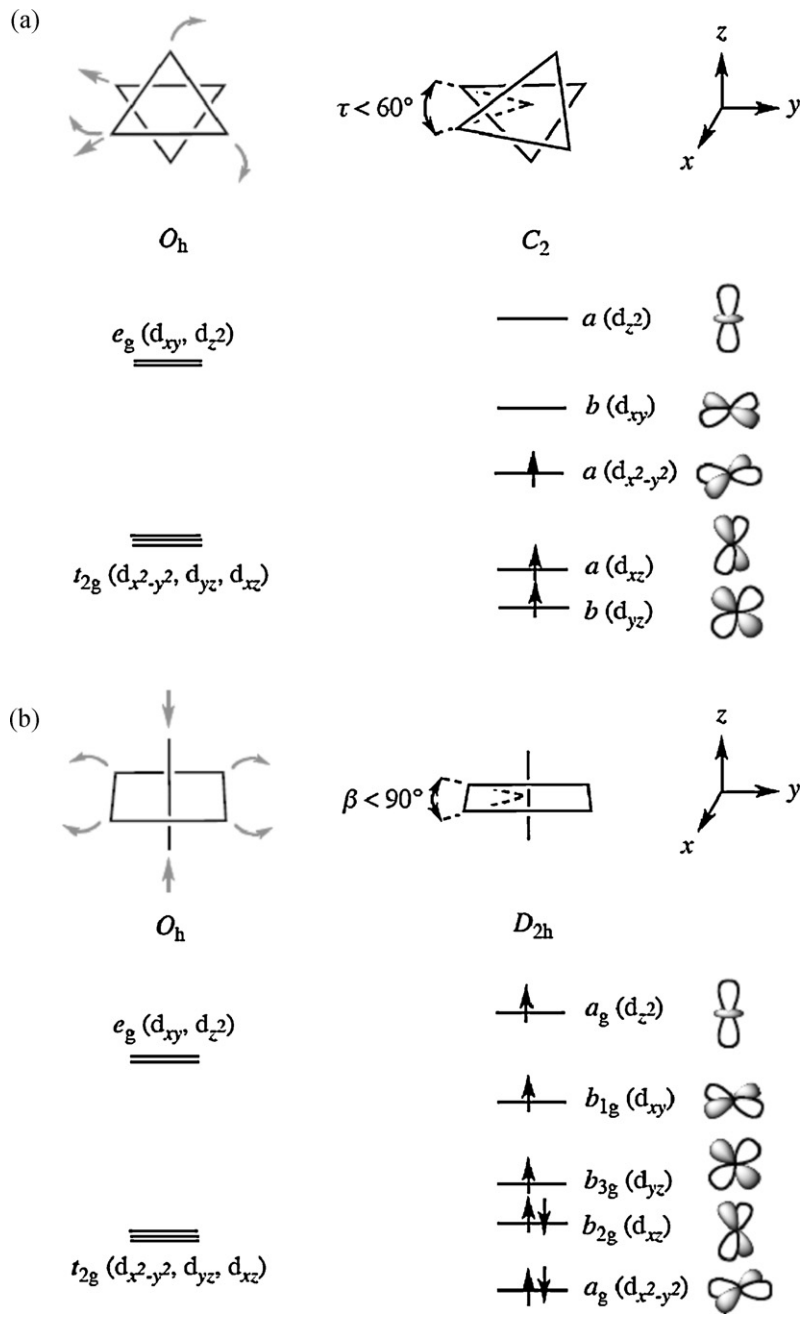

Scheme 5.

fit of the magnetic data through Eqs. (1)–(3) gives $|D| = 0.2\ cm^{-1}$; $\theta = -0.5$ K.

4. Oligonuclear complexes

The self-assembly process involving the $[Cr(AA)(C_2O_4)_2]^-$ building block and first-row transition metal ions represents a successful strategy to prepare heterobimetallic complexes. The assembling cations can be either (a) fully solvated metal ions, in which one, two or all the solvent molecules can be replaced by the bridging oxalato groups, or (b) preformed cationic complexes with blocking ligands and weakly bonded solvent molecules in the coordination sphere of the metal ion. The stereochemical preference of the assembling cation, as well as the presence of the ancillary ligands play a crucial role on the nuclearity and the topology of the resulting heterobimetallic complexes.

4.1. Dinuclear heterobimetallic Cr(III)–Mn(III), Cr(III)–Cu(II) and Cr(III)–Mn(II) complexes

The formation of binuclear complexes is favoured by monopositively charged assembling cations, with the metal ion chelated by ligands with denticity higher than 2, or by two bidentate ligands.

Two oxalato-bridged Cr(III)–Mn(III) binuclear complexes, $[\{Mn(H_2O)(valen)\}\{Cr(AA)(C_2O_4)_2\}]\cdot 3H_2O$ [AA = bipy (**6a**) and phen (**6b**)] were obtained by reacting the mononuclear manganese(III) precursor, $[Mn(valen)(H_2O)(MeCN)]ClO_4$ with $AsPh_4[Cr(AA)(C_2O_4)_2]$ (H_2valen is a bicompartmental Schiff-base proligand, resulting from the 2:1 condensation of 3-methoxysalicyladehyde with ethylenediamine [24]). In the two compounds the $[Cr(AA)(C_2O_4)_2]^-$ ions coordinate through one oxalato oxygen atom into one apical position of the manganese(III) ions. Fig. 5 illustrates the molecular structure of **6a**. The values of the intramolecular distance between the metal centres across the

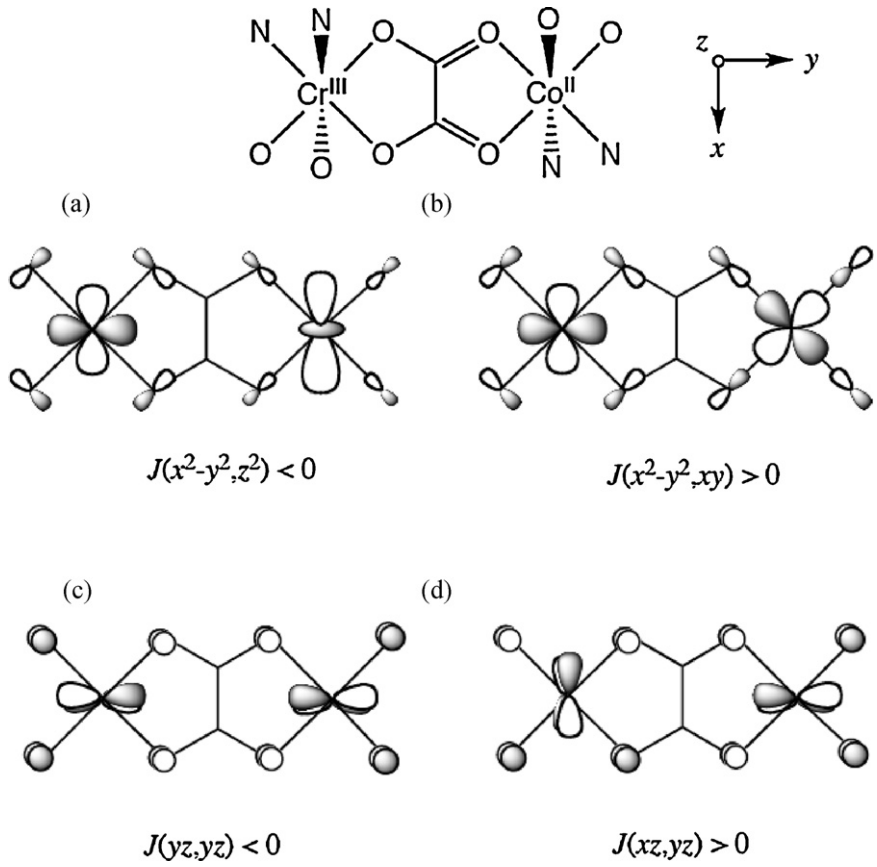

Scheme 6.

bidentate/monodentate (outer) oxalato bridge are 5.329 (**6a**) and 5.442 Å (**6b**).

A binuclear Cr(III)–Cu(II) complex, [{Cu(Hfsaaep)}{(Cr(bipy)(C_2O_4)$_2$}]·2H_2O **7** [25], has been obtained by reacting Na[Cr(bipy)(C_2O_4)$_2$] with the binuclear chloro-bridged copper(II) complex, [Cu(Hfsaaep)Cl]$_2$ [H_2fsaaep is a Schiff-base ligand derived from 3-formylsalicylic acid and 2-(2aminoethyl)pyridine]. The chloro ligand in the {Cu(Hfsaaep)Cl} moiety was substituted by the [Cr(bipy)(C_2O_4)$_2$]$^-$ unit, resulting in a neutral [$Cu^{II}Cr^{III}$] heterodinuclear complex (Fig. 6a). The [Cr(bipy)(C_2O_4)$_2$]$^-$ ion acts as a bidentate ligand towards the copper(II) ion, that is, one of the two oxalato groups adopts the bis-bidentate coordination mode. The distance between the oxalato-bridged Cr(III) and Cu(II) ions is 5.506 Å. The environment of the copper(II) ion is elongated octahedral, with the axial positions being occupied by an oxalato oxygen [Cu(1)–O(4) = 2.504(2) Å] and a water molecule [Cu(1)–O(1w) = 2.360(3) Å]. The phenolic group of the Schiff-base ligand is deprotonated, while the carboxylic group remains protonated. The packing of the molecules in the crystal is driven by two organizing forces: (i) hydrogen bonds established between the water molecule coordinated to copper(II), the oxygen atoms from the terminal oxalate group, and the crystallization water molecules (Fig. 6b); and (ii) π–π stacking interactions between the bipy ligands from neighboring supramolecular chains constructed from hydrogen-bonded binuclear complexes (Fig. 6c).

From the magnetic point of view, the Cu(II)–Cr(III) pair represents a classical case of orthogonality of the magnetic orbitals that leads to a ferromagnetic coupling (if the symmetry conditions are fulfilled). Indeed, below 50 K the $\chi_M T$ product of **7** increases, indicating a ferromagnetic interaction between the oxalato-bridged Cu(II) and Cr(III) ions (Fig. 7). The energies of the low-lying spin states for the Cu(II)(S = 1/2)–Cr(III)(S = 3/2) pair are obtained using the isotropic spin Hamiltonian: $\boldsymbol{H} = -JS_{Cu}S_{Cr}$, ($J$ is the exchange coupling parameter, and S_{Cu} and S_{Cr} are the operators associated to the local spins) which leads to the following expression describing the temperature dependence of the $\chi_M T$ product [Eq. (4)]:

$$\chi_M T = \frac{2N\beta^2}{k}\frac{5g_2^2 + g_1^2 e^{-2J/kT}}{5 + 3e^{-2J/kT}} \quad (4)$$

where $g_1 = (5g_{Cr} - g_{Cu})/4$; $g_2 = (3g_{Cr} + g_{Cu})/4$. Least-squares fit to the data leads to the following values: J = +1.4 cm^{-1}, g_{Cr} = 1.99 and g_{Cu} = 2.10. This ferromagnetic interaction was previously observed with other oxalato-bridged Cr(III)–Cu(II) complexes [3b,c] constituting thus suitable examples of ferromagnetic coupling through strict orthogonality of the interacting magnetic orbitals ($t_{2g}^3 e_g^0$ versus $t_{2g}^6 e_g^3$ electronic configurations for ocatahedral Cr(III) and Cu(II) ions, respectively).

Two other binuclear Cu(II)–Cr(III) complexes of formula [{Cu(bpca)}{Cr(AA)(C_2O_4)$_2$}]·$n$$H_2O$ have resulted by assembling [Cu(bpca)]$^+$ and [Cr(AA)(C_2O_4)$_2$]$^-$ ions [Hbpca = bis(2-pyridylcarbonyl)amide and AA = bipy with n = 2.5 (**8a**) or phen with n = 2 (**8b**)] [13]. The structure of **8b** is shown in Fig. 8. The anionic building block is coordinated to the copper(II) ion through only one oxalato oxygen which occupies the apical position of the square-pyramidal environment at the copper(II) center (three nitrogen atoms from the bpca ligand and a water molecule building the basal plane). The magnetic orbital of the copper(II) (d_{x2-y2}) is located in the basal plane, the spin density on the apical oxalato oxygen atom being very weak. Consequently, the

predicted lack of significant overlap between the magnetic orbitals of the two metal ions through this equatorial (at the chromium) apical (at the copper) exchange pathway, which is provided the bidentate/monodentate (outer) oxalate bridge, accounts for the negligible intramolecular magnetic coupling in **8a**. The observed decrease of the $\chi_M T$ product below 10 K for both **8a** and **8b** (the two compounds have the same type of oxalato bridge) is due to the zero field splitting of chromium(III) ion.

Finally, a heterobimetallic Mn(II)–Cr(III) dinuclear complex of formula $[\{Mn(phen)_2(N_3)\}\{Cr(phen)(C_2O_4)_2\}]\cdot H_2O$ **9** was obtained by blocking five out of the six coordination sites of the manganese(II) ion with one azido and two phenanthroline ligands [25]. Its crystal structure is depicted in Fig. 9. The $[Cr(phen)(C_2O_4)_2]^-$ ion acts as a monodentate ligand through an oxalato oxygen atom towards the $[Mn(phen)_2(N_3)]^+$ moiety. The intramolecular Cr···Mn distance is 5.257 Å. The manganese(II) ion is six-coordinated by five nitrogen atoms, four of them from two phen molecules and the other one from an azido ligand, plus one oxygen atom from the bridging oxalato group. The magnetic data for this compound were a spin sextuplet [Mn(II)($S = 5/2$)] and a spin quartet [Cr(III)($S = 3/2$)] are involved, were fitted by the expression derived through the isotropic Hamiltonian $\boldsymbol{H} = -JS_{Mn}S_{Cr}$, [Eq. (5)]:

$$\chi_M T = \frac{2N\beta^2 g^2}{k} \frac{e^{-21J/4kT} + 5e^{-13J/4kT} + 14e^{-J/4kT} + 30e^{15J/4kT}}{3e^{-21J/4kT} + 5e^{-13J/4kT} + 7e^{-J/4kT} + 9e^{15J/4kT}} \quad (5)$$

where a common Landé factor (g) was assumed for the two metal ions. The exchange interaction between the Mn(II) and Cr(III) in **9** was antiferromagnetic ($J = -1.9\,cm^{-1}$). In this case, the presence of five unpaired electrons on the Mn(II) ion (five magnetic orbitals) increases the possibility of net overlap with the three magnetic orbitals at the Cr(III) and then an antiferromagnetic coupling is predicted, as observed.

4.2. Trinuclear heterometallic complexes

The first trinuclear heterometallic complexes obtained by assembling the bis-oxalato building blocks and hydrated cations were $[\{Co(H_2O)_2\}\{Cr(bipy)(C_2O_4)_2\}_2]\cdot H_2O$ **10** [26], $[\{Ni(H_2O)_2\}\{Cr(bipy)(C_2O_4)_2\}_2]\cdot H_2O$ **11** [27], and $[\{Cu(H_2O)_2\}\{Cr(bipy)(C_2O_4)_2\}_2]\cdot 1.5H_2O$ **12** [28]. Compounds **10** and **11** were synthesized by reacting the barium derivative, $Ba[Cr(bipy)(C_2O_4)_2]_2$ with the corresponding transition metal sulfate, while **12** was prepared by reacting copper(II) nitrate with $K[Cr(bipy)(C_2O_4)_2]$. Compounds **10** and **12** are isomorphous and their structures consist of neutral, centrosymmetric trinuclear species (Fig. 10). Each $[Cr(bipy)(C_2O_4)_2]^-$ anion is coordinated to the central ion through the outer oxygen atoms of one oxalato group (bis-bidentate bridging mode). The central metal ion [Cu(II) or Co(II)] is six-coordinated, with an elongated octahedral geometry, two aqua ligands being disposed in *trans* positions. Because of the strong preference of Ni(II) for the octahedral stereochemistry, compound **11** is most likely isostructural with **10** and **12**. The elongation of the coordination octahedron for Cu(II) in **12** along the O3CuO3A axis is more important than in the case of the Co(II) ion in **10** due to the Jahn–Teller effect:

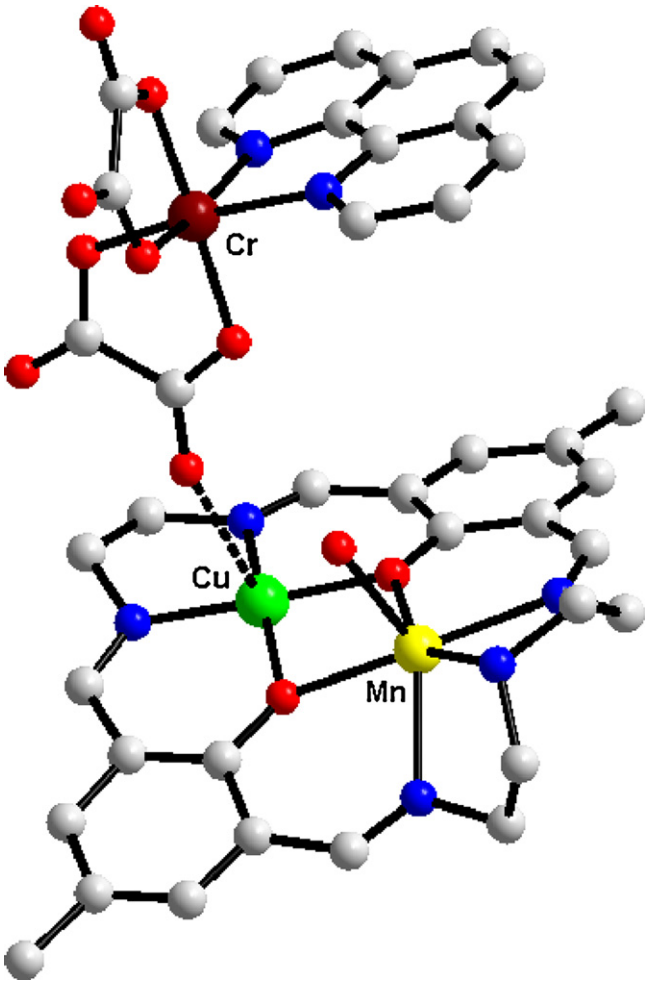

Fig. 13. View of the heterotrimetallic $[\{LCuMn(H_2O)\}\{Cr(phen)(C_2O_4)_2\}]^+$ cation in **14**.
Adapted from Ref. [30].

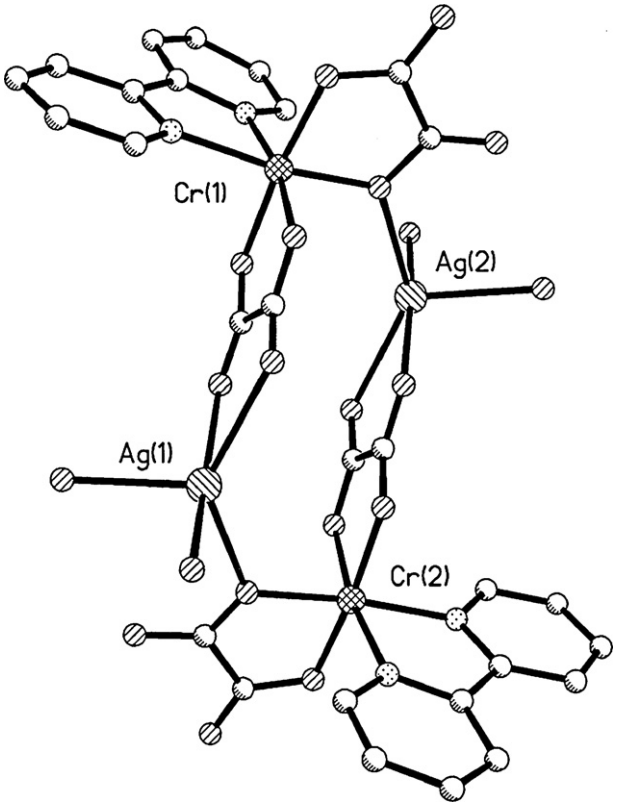

Fig. 14. Molecular structure of $[\{Ag(H_2O)\}\{Cr(bipy)(C_2O_4)_2\}]_2$ **15**.
Adapted from Ref. [28].

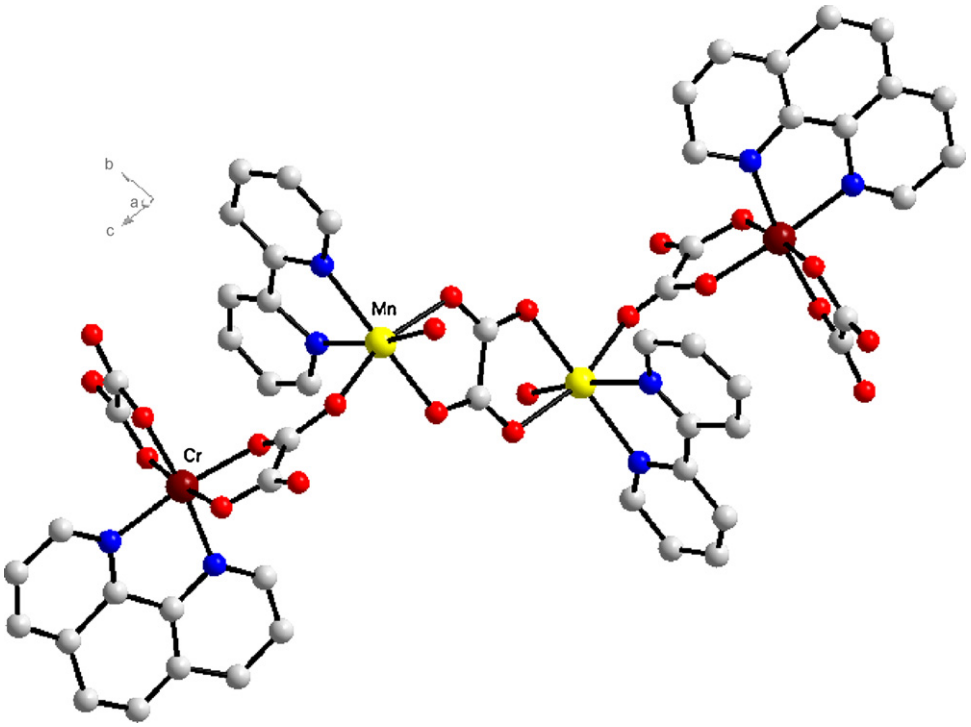

Fig. 15. Perspective view of the neutral Cr(III)–Mn(II)–Mn(II)–Cr(III) tetranuclear unit of complex **16**. Adapted from Ref. [14].

Cu–O1 = 1.953(4) Å Co–O1 = 2.057(9) Å

Cu–O2(ox) = 1.998(3) Å Co–O2(ox) = 2.089(6) Å

Cu–O3(ox) = 2.357(3) Å Co–O3(ox) = 2.155(6) Å

The unpaired electron of the copper(II) ion (the magnetic orbital) is mainly localized in the O1O2O1AO2A plane that is in a plane which is perpendicular to that of the bridging oxalato. Under this orientation, a net overlap is expected between the magnetic orbital of the Cu(II) and those of the Cr(III) and consequently, the intramolecular exchange interaction in complex **12** is predicted to be antiferromagnetic. For a ABA trinuclear complex with $S_A > S_B + 1$ (S_A and S_B being the local spins) an irregular spin state structure results, and the $\chi_M T$ versus T curve exhibits a minimum [1,4b].

In principle, the complexes with the general formula $[\{M(H_2O)_2\}\{Cr(bipy)(C_2O_4)_2\}_2]$ (M being a divalent transition metal ion with an octahedral coordination geometry) can exhibit two topologies: either linear, when the aqua ligands are coordinated in *trans*, or angular when the aqua ligands are bound in *cis* positions. If the bivalent metal ion carries a bidentate ligand instead of two aqua ligands, then only the angular configuration is possible (Scheme 4). Indeed, the reactions between $PPh_4[Cr(AA)(C_2O_4)_2]$ and $[Co(6,6'\text{-dmbipy})(H_2O)_4](NO_3)_2$ (prepared *in situ* from a 1:1 mixture of $Co(NO_3)_2{\cdot}6H_2O$ and 6,6′-dimethyl-2,2′-bipyridine in methanol) afforded two heterotrinuclear complexes: $[\{Co(6,6'\text{-dmbipy})\}\{Cr(AA)(C_2O_4)_2\}_2]{\cdot}nH_2O$ [AA = bipy with $n = 2$ (**13a**) and phen with $n = 1.5$ (**13b**)] [29]. The crystal structure of **13b** confirms the expected angular geometry of the neutral complex (Fig. 11). The value of the intramolecular Cr1···Co1···Cr2 angle is 104.83(3)° and those of the intramolecular Cr1···Co1 and Cr2···Co1 distances across the oxalato bridges are 5.332 and 5.372 Å, respectively. The investigation of the magnetic properties for **13a** and **13b** reveals a ferromagnetic coupling between the central Co(II) ion and the peripheral Cr(III) ions (Fig. 12).

In general, the six-coordinated octahedral high-spin Co(II) ion presents an important first-order orbital momentum, so that the spin Hamiltonian is insufficient to treat the magnetic properties of polynuclear cobalt(II) complexes and it must be supplemented by consideration of orbitally dependent exchange interactions as well as spin–orbit coupling (SOC) effects. However, the first-order SOC effects of the orbitally degenerate high-spin d^7 Co(II) ion ($S_{Co} = 3/2$ and $L_{Co} = 1$) can be conveniently neglected in **13a** and **13b** because of the important distortions from the ideal octahedron, as shown by the crystal structure of **13b**. Consequently, the analysis of the magnetic susceptibility data of **13a** and **13b** was first carried out through the spin Hamiltonian for a trinuclear model that only takes into account the presence of weak intermolecular interactions within

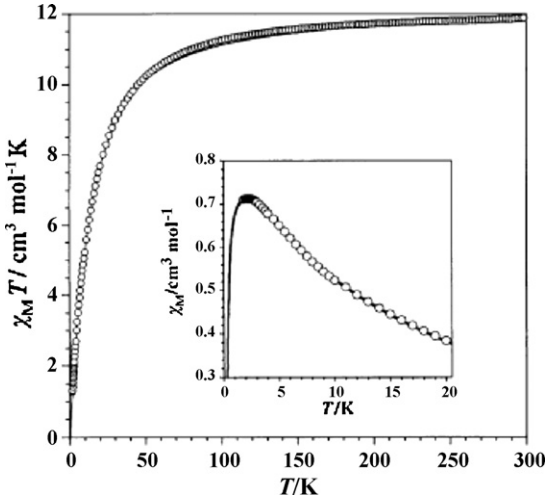

Fig. 16. $\chi_M T$ versus T curve for compound **16**. Adapted from Ref. [14].

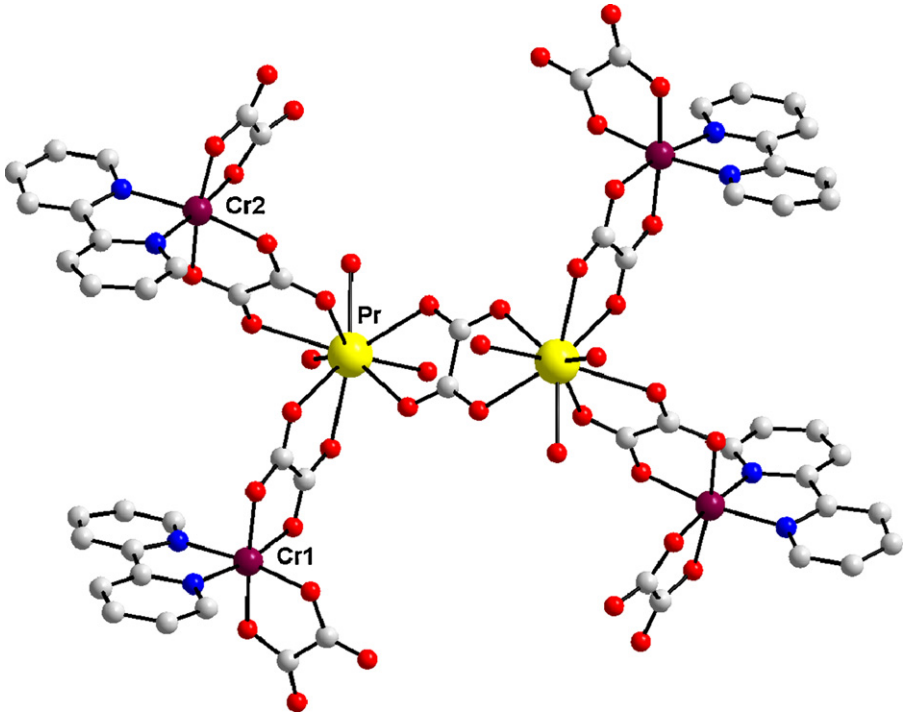

Fig. 17. Crystal structure of the hexanuclear complex, $[Pr^{III}_2Cr^{III}_4]$ **17**.
Adapted from Ref. [32].

the mean field approximation [Eq. (6) with $S_{Co1} = S_{Cr1} = S_{Cr2} = 3/2$]:

$$\boldsymbol{H} = -J(S_{Co1} \times S_{Cr1} + S_{Co1} \times S_{Cr2}) + zj < S_z > S_z \quad (6)$$

where J and zj are the intra- and intermolecular magnetic coupling parameters respectively, and g_{Co} and g_{Cr} are the Landé factors of the Co(II) and Cr(III) ions. The least-squares fit of the experimental data through the appropriate expression [Eq. (7), where $x = J/k_BT$ and θ is the Weiss factor defined as $\theta = zjS(S+1)/3k_B$ with $S = 9/2$] gave $J = +2.47\ cm^{-1}$, $zj = -0.14\ cm^{-1}$, $g_{Co} = 2.075$, and $g_{Cr} = 2.012$ for **13a**, and $J = +2.37\ cm^{-1}$, $zj = -0.11\ cm^{-1}$, $g_{Co} = 2.091$, and $g_{Cr} = 2.011$ for **13b**.

$$\chi_M = \left[\frac{N\beta^2}{12k_B(T-\theta)}\right]\left(\frac{A}{B}\right) \quad (7)$$

with

$$A = \left(\frac{165}{3}\right)(2g_{Cr} + g_{Co})^2 + \left(\frac{36}{7}\right)(4g_{Cr} + 3g_{Co})^2 \exp\left(-\frac{3x}{2}\right) + \left(\frac{21}{5}\right)(3g_{Co} + 2g_{Cr})^2 \exp(-3x) + 30g_{Co}^2 \exp\left(-\frac{9x}{2}\right) + \left(\frac{12}{21}\right)(16g_{Cr} + 5g_{Co})^2 \exp\left(-\frac{9x}{2}\right)$$

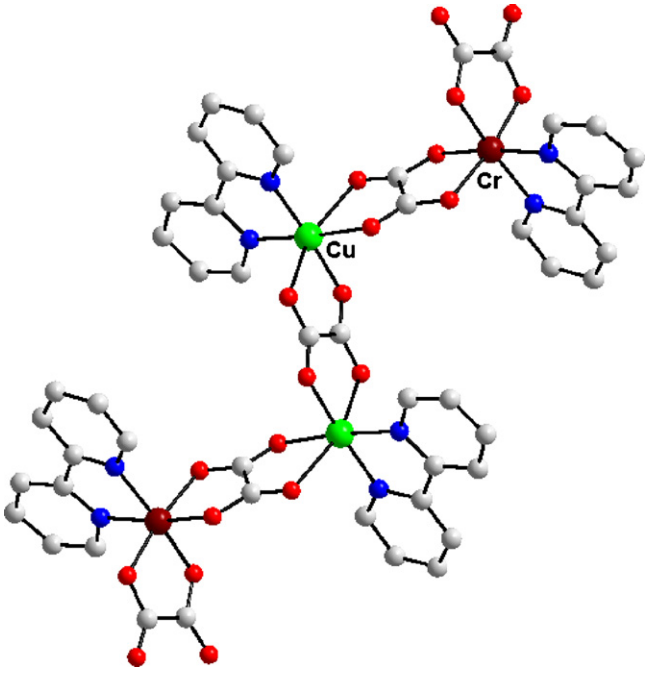

Fig. 18. Molecular structure of $[\{Cu(bipy)\}_2(C_2O_4)\{Cr(bipy)(C_2O_4)_2\}_2]\cdot 2H_2O$ **18**.
Adapted from Ref. [33].

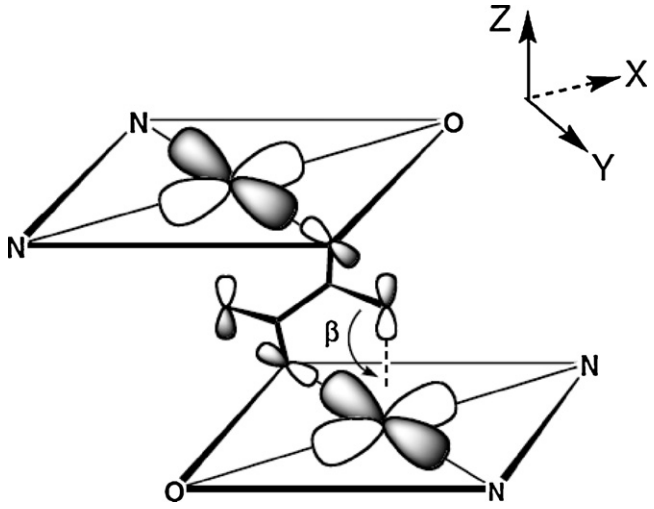

Scheme 7.

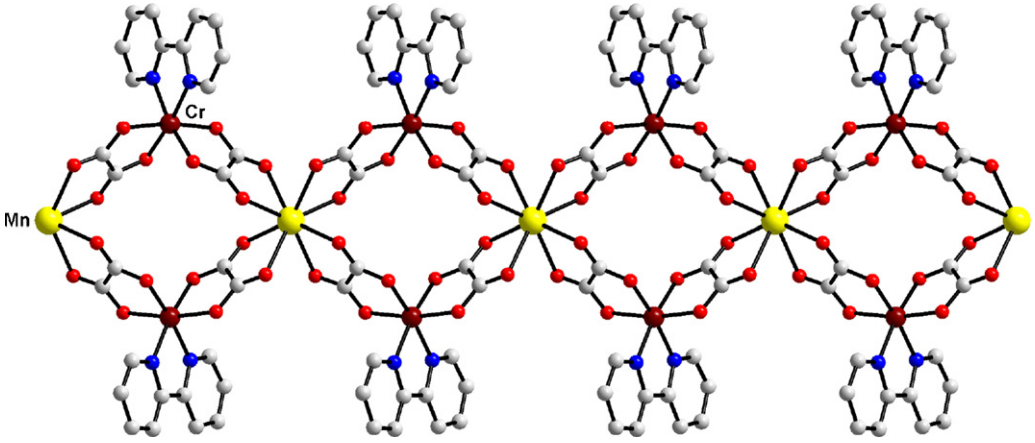

Fig. 19. Perspective view of one enantiomeric chain in ${}_1{}^{\infty}[Mn\{Cr(bipy)(C_2O_4)_2\}_2]_n$ **19**.
Adapted from Ref. [26].

$$+\left(\frac{3}{35}\right)(22g_{Cr}+13g_{Co})^2\exp(-5x)$$
$$+\left(\frac{2}{15}\right)(11g_{Co}+4g_{Cr})^2\exp\left(-\frac{11x}{2}\right)$$
$$+\left(\frac{1}{3}\right)(5g_{Co}-2g_{Cr})^2\exp(-7x)+\left(\frac{6}{5}\right)(4g_{Cr}+g_{Co})^2$$
$$\times\exp\left(-\frac{15x}{2}\right)+\left(\frac{3}{35}\right)(34g_{Cr}+g_{Co})^2\exp(-8x)$$
$$+3(2g_{Cr}-g_{Co})^2\exp(-9x)+\left(\frac{6}{5}\right)(8g_{Cr}-3g_{Cr})^2\exp\left(-\frac{21x}{2}\right)$$

and

$$B=5+4\exp\left(-\frac{3x}{2}\right)+3\exp(-3x)+6\exp\left(-\frac{9x}{2}\right)$$
$$+3\exp(-5x)+2\exp\left(-\frac{11x}{2}\right)+\exp(-7x)+2\exp\left(-\frac{15x}{2}\right)$$
$$+3\exp(-8x)+\exp(-9x)+2\exp\left(-\frac{21x}{2}\right)$$

An alternative analysis of the magnetic susceptibility data of **13a** and **13b** was carried out through the appropriate spin Hamiltonian for a trinuclear system that also takes into account the local axial ZFS of the orbital singlet ${}^4B_{2g}$ ground state of the high-spin Co(II) ion in a rhombically distorted octahedral geometry (D_{2h} point group) [Eq. (8)] with $S_{Co1}=S_{Cr1}=S_{Cr2}=3/2$:

$$\boldsymbol{H}=-J(S_{Co1}\times S_{Cr1}+S_{Co1}\times S_{Cr2})+zj<S_z>S_z+D_{Co}S_{Co1z}^2 \quad (8)$$

where J and zj are the intra- and intermolecular magnetic coupling parameters respectively, D_{Co} is the axial magnetic anisotropy parameter of the Co(II) ion, and g_{Co} and g_{Cr} are the Landé factors of the Co(II) and Cr(III) ions. The least-squares fit of the experimental data by full-matrix diagonalization techniques gave $J=+2.43\,cm^{-1}$, $zj=-0.12\,cm^{-1}$, $D_{Co}=-2.29\,cm^{-1}$, $g_{Co}=2.091$, and $g_{Cr}=1.998$ for **13a**, and $J=+2.34\,cm^{-1}$, $zj=-0.08\,cm^{-1}$, $D_{Co}=-2.15\,cm^{-1}$, $g_{Co}=2.089$, and $g_{Cr}=2.009$ for **13b**.

The relatively large axial magnetic anisotropy of the central high-spin Co^{II} ion for **13a** ($D_{Co}=-2.29\,cm^{-1}$) and **13b** ($D_{Co}=-2.15\,cm^{-1}$) agrees with the rather important structural distortions from the ideal octahedral metal environment.

The moderately weak ferromagnetic intramolecular coupling between the two peripheral Cr^{III} ions and the central high-spin Co^{II} ion for **13a** ($J=+2.43\,cm^{-1}$) and **13b** ($J=+2.34\,cm^{-1}$) suggests that the exchange interaction involves a subtle competition between σ- and π-orbital pathways across the oxalato bridge (spin delocalization mechanism). As a matter of fact, the overall magnetic coupling parameter (J) for metal ions with more than one unpaired electron can be decomposed into a sum of individual exchange coupling contributions (J_{ij}) involving each pair of magnetic orbitals according to $J=(1/n_A)(1/n_B)\sum_{i,j}J_{ij}$, where n_A and n_B are the number of unpaired electrons per metal center [$n_A=n_B=3$ for A = Cr(III) and B = Co(II)]. That being so, the nature and magnitude of the magnetic coupling (J) ultimately depend on the nature and magnitude of each individual contribution, which can be either ferro- ($J_{ij}>0$) or antiferromagnetic ($J_{ij}<0$) for an orthogonal or nonorthogonal pair of magnetic orbitals, respectively. So, the d^3 Cr(III) ion in a trigonal distorted trapezoidal bipyramidal geometry (${}^4B$ ground term in the C_2 point group) possesses three unpaired electrons occupying the a ($d_{x^2-y^2}$), a (d_{xz}), and b (d_{yz}) magnetic orbitals resulting from the splitting of the t_{2g} (d_{xz}, d_{yz}, $d_{x^2-y^2}$) level because of the combined effect of trigonal twist and *cis* equatorial elongation (Scheme 5a). By contrast, the three unpaired electrons of the high-spin d^7 Co(II) ion in a compressed rectangular bipyramidal geometry (${}^4B_{2g}$ ground term in the D_{2h} point group) occupy the a_g (d_{z^2}), b_{1g} (d_{xy}), and b_{3g} (d_{yz}) magnetic orbitals resulting from the splitting of the e_g (d_{z^2}, d_{xy}) and t_{2g} (d_{xz}, d_{yz}, $d_{x^2-y^2}$) levels due

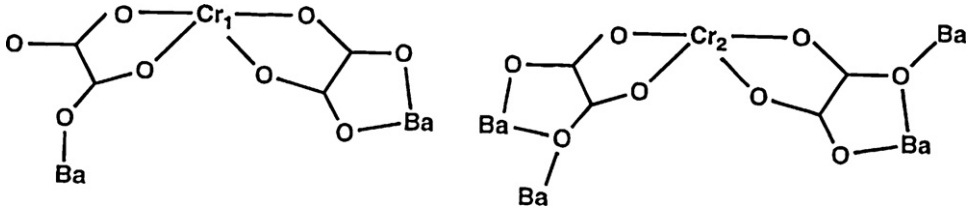

Scheme 8.

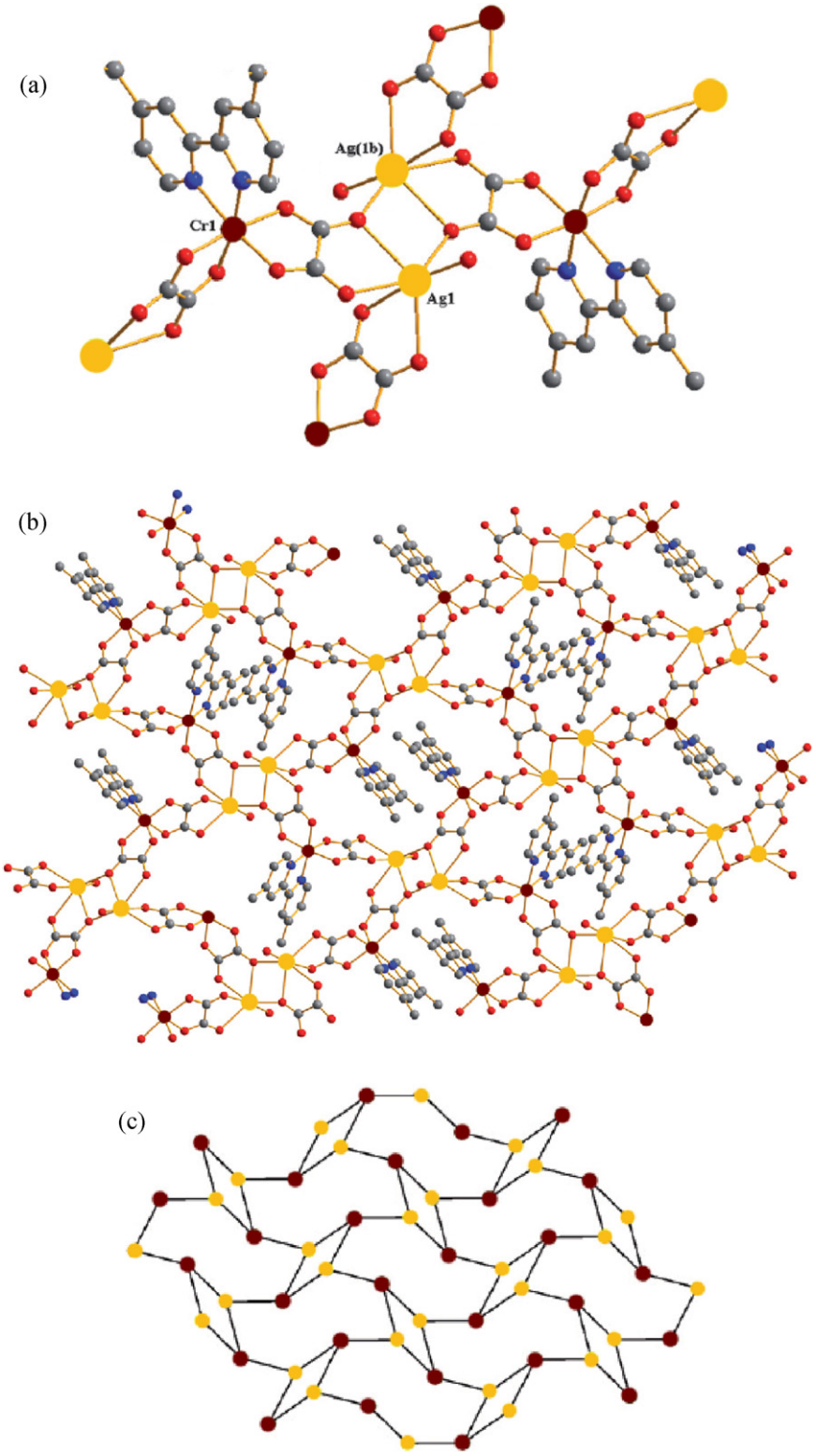

Fig. 20. Construction of 2D layers in compounds **20**–**23**; (a) detail of the crystal structure of **22**, showing the interaction of the oxalato ligand with the silver atoms; (b) view of the bimetallic layer showing the $Cr(III)_4Ag(I)_4$ holes filled by the chelating dmbipy ligands in **22**; (c) view of the topological layer in compounds **21**–**23**. Adapted from Refs. [12,14,17,36].

to the combined effect of axial compression and equatorial bending (Scheme 5b). This situation gives rise to $3 \times 3 = 9$ individual exchange coupling contributions for each oxalato-bridged $Cr^{III}Co^{II}$ pair unit. Restricting ourselves to the purely σ- or π-type orbital contributions across the oxalato bridge (Scheme 6), the J value of **13a** and **13b** can be calculated according to $J = (1/9)(J_{x^2-y^2,z^2} + J_{yz,yz} + J_{xz,yz})$. Hence, the ferromagnetic coupling observed in these oxalato-bridged chromium(III)–cobalt(II) complexes is explained

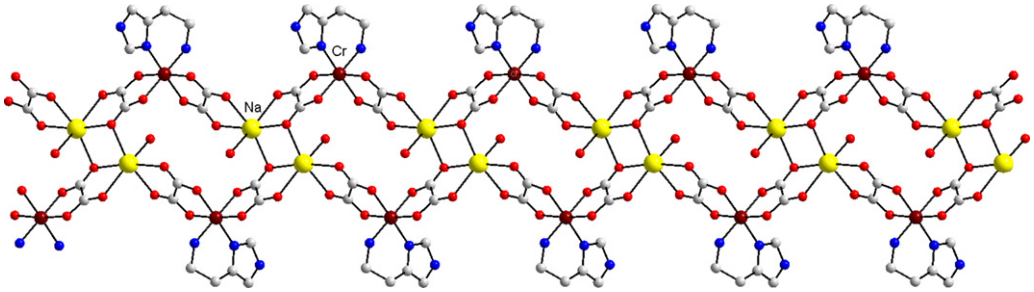

Fig. 21. View of a chain in $_1{}^{\infty}[\{Na(H_2O)\}\{Cr(hm)(C_2O_4)_2\}]\cdot 2H_2O$ **24**.
Adapted from Ref. [37].

by the larger magnitude of the positive ferromagnetic contributions ($J_{x^2-y^2,xy}$ and $J_{xz,yz} > 0$) with a zero orbital overlap (Scheme 6b and d) compared to the negative antiferromagnetic ones ($J_{x^2-y^2,z^2}$ and $J_{yz,yz} < 0$) with a nonzero orbital overlap (Scheme 6a and c).

The $[Cr(AA)(C_2O_4)_2]^-$ ion can be involved in the stepwise synthesis of heterotrimetallic compounds (complexes with three different metal ions within the same molecular entity). This is possible when the assembling cation is a heterobimetallic species. Such a trimetallic complex of formula $[\{LCuMn(H_2O)\}\{Cr(phen)(C_2O_4)_2\}]ClO_4\cdot H_2O$ (**14**) (Fig. 13) has been obtained by reacting $[L^1CuMn(H_2O)](ClO_4)_2$ with $K[Cr(phen)(C_2O_4)_2]$ (H_2L^1 is a bicompartmental Schiff-base resulting from the stepwise condensation of 2,6-diformyl-*p*-cresol with ethylenediamine and diethylenetriamine [30]. The copper(II) and manganese(II) ions in **14** are hosted into the compartments of the macrocyclic ligand. The bis-oxalato chromium complex acts as a monodentate ligand towards the copper(II) ion through one oxygen atom filling the apical position at the copper(II) ion. This apical coordination of the oxalato ligand accounts for the weak, if any, magnetic coupling between the chromium(III) and the copper(II) ions in this trimetallic compound.

4.3. Tetra- and hexanuclear heterobimetallic complexes

A tetranuclear $[Ag^I{}_2Cr^{III}{}_2]$ complex [28] with a surprising structure was obtained through the transmetallation reaction:

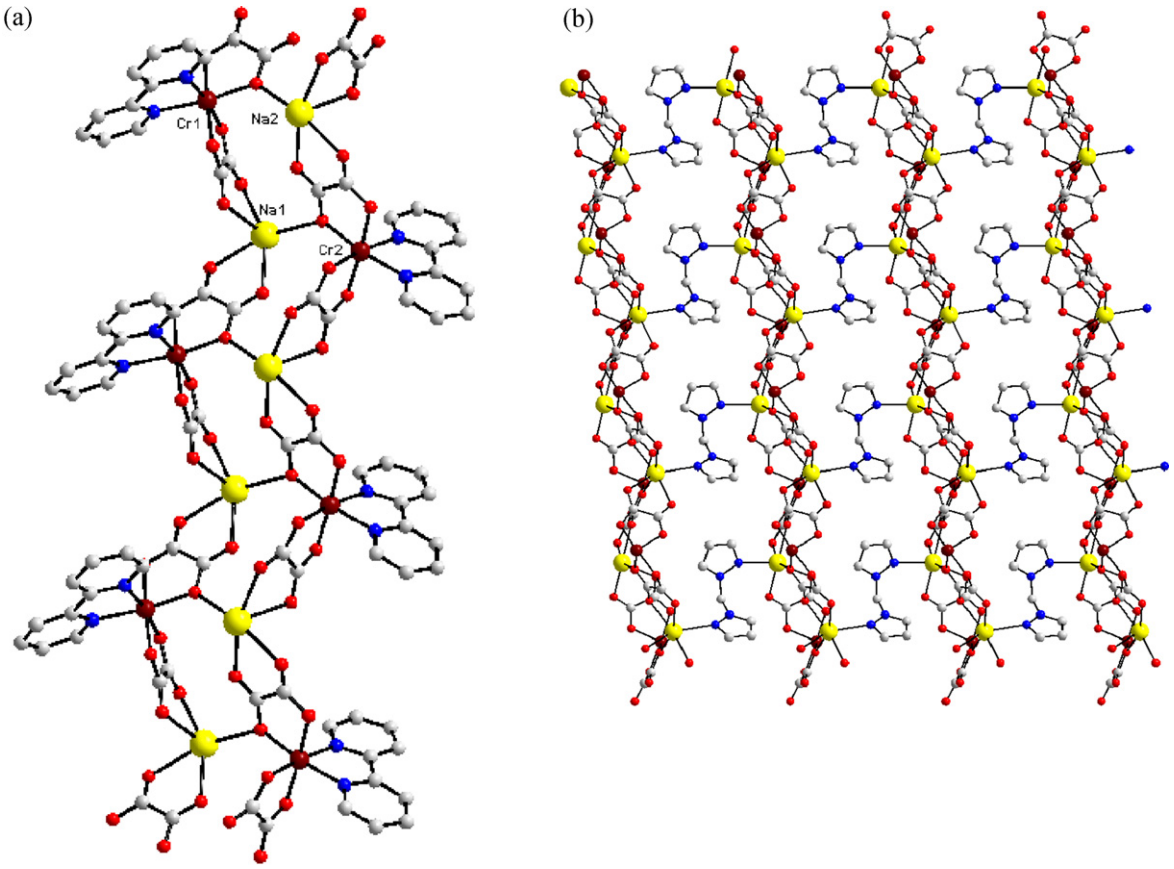

Fig. 22. (a) Formation of the bimetallic chains in $_2{}^{\infty}[\{Na(bpm)\}Cr(bipy)(C_2O_4)_2]\cdot 2H_2O$ **25**, by connecting the sodium and chromium ions through oxalato bridges. For the sake of clarity, the bpm spacers have been removed. (b) Perspective view of the 2D coordination polymer, resulted by connecting the bimetallic chains with bpm spacers. For the sake of clarity, the bipy ligands attached to the chromium ions are not represented.
Adapted from Ref. [38].

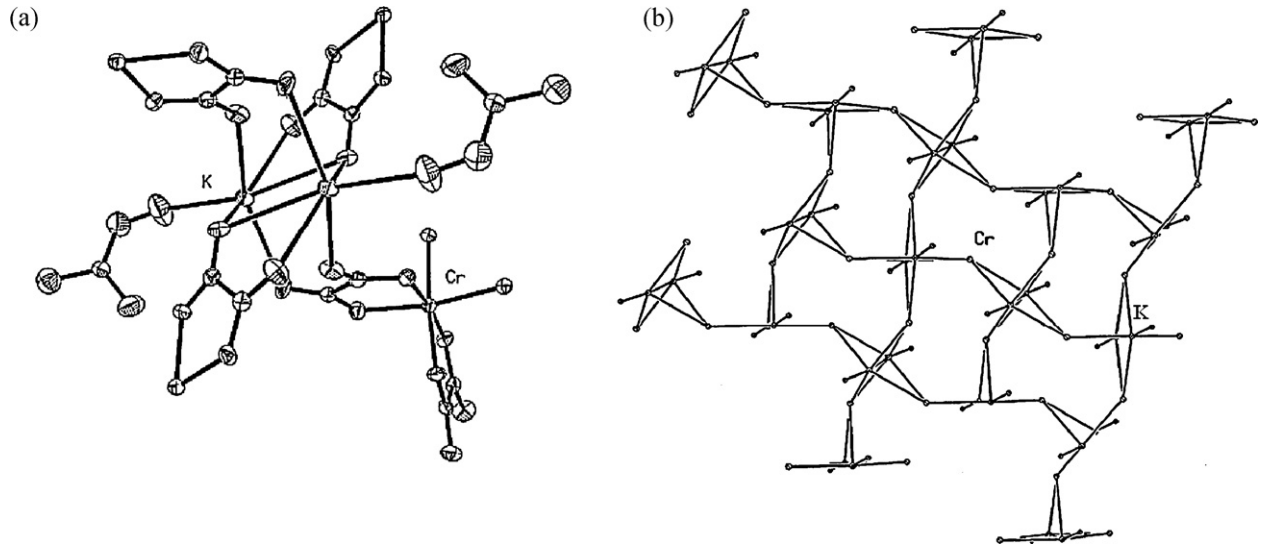

Fig. 23. Construction of a 2D layer in compound **26**; (a) detail of the crystal structure showing the interaction of the oxalate groups with the potassium ions; (b) view of a layer showing only the chromium and potassium atoms.
Adapted from Ref. [18].

$$Ba[Cr(bipy)(C_2O_4)_2]_2 + Ag_2SO_4 \rightarrow \underset{\mathbf{15}}{[\{Ag(H_2O)\}\{Cr(bipy)(C_2O_4)_2\}]_2} + BaSO_4$$

The structure of **15** consists of discrete neutral metallacycles formed by two chromium(III) and two silver(I) ions bridged by oxalato groups (Fig. 14). The chiral chromium coordinated centers within a tetranuclear entity have opposite absolute configurations. Two of the oxalato groups exhibit their commonest bis-chelating coordination mode (bis-bidentate) while the other two exhibit the bidentate/monodentate (inner) bridging mode. The silver(I) ions are five-coordinated with a distorted trigonal bipyramidal geometry. The values of the intramolecular Cr···Ag distances are 3.841 and 3.886 Å [through the bidentate/monodentate (inner) oxalato] and 5.749 and 5.719 Å (across bis-bidentate oxalato).

The reaction between $Na[Cr(phen)(C_2O_4)_2]\cdot 3H_2O$, manganese(II) chloride tetrahydrate, 2,2′-bipyridine and sodium oxalate in a 1:1:1:0.5 molar ratio in aqueous solution afforded an interesting tetranuclear complex of formula $[\{Mn(bipy)(H_2O)\}_2(C_2O_4)\{Cr(phen)(C_2O_4)_2\}_2]\cdot 6H_2O$ **16** [14]. The central manganese(II) ions are bridged by a bis-bidentate oxalato ligand (Fig. 15). Each $[Cr(phen)(C_2O_4)_2]^-$ unit in **16** acts as a monodentate ligand through only one oxalate oxygen atom towards the manganese(II) ions. Three different coordination modes of the oxalato ligands are observed within this complex: the usual bis-bidentate [between the manganese(II) ions], bidentate [at the peripheral chromium(III) ions] and simultaneously bidentate [towards the chromium(III)] and monodentate outer [towards manganese(II)]. The peripheral chromium moieties are *trans* with respect to the central μ-oxalato-bis[aqua(2,2′-bipyridine)manganese(II)] unit.

Two main exchange pathways, both across the oxalato bridges, dictate the magnetic behavior of **16**: the magnetic coupling between the central manganese(II) ions, and that between each manganese(II) center and the peripheral chromium(III) ion. The isotropic exchange Hamiltonian that applies for such a system is given by Eq (9):

$$\boldsymbol{H} = -J_1 S_{Mn1} S_{Mn2} - J_2 (S_{Cr1} S_{Mn1} + S_{Cr2} S_{Mn2}) \quad (9)$$

The $\chi_M T$ versus T curve for **16** (Fig. 16) indicates an overall antiferromagnetic behaviour. The best fit to the data is achieved with the parameters $J_1 = -2.2\,cm^{-1}$ and $J_2 = -1.1\,cm^{-1}$. The first value remains within the range of those previously reported for magneto-structurally characterized examples of oxalato-bridged dimanganese(II) complexes (J values covering the range -1.8 to $-2.5\,cm^{-1}$) [31]. The last value is close to the one found for the similar Mn(II)–(μ-oxalato)-Cr(III) dinuclear complex **9** ($J = -1.9\,cm^{-1}$) [25].

The partial decomposition of the chromium building blocks can generate interesting compounds as well. For example, the reaction between $Na[Cr(bipy)(C_2O_4)_2]$ and $LnCl_3$ (Ln = Pr and Gd) afforded the hexanuclear $[Ln^{III}_2Cr^{III}_4]$ complexes, $[\{Ln(H_2O)_3\}_2(C_2O_4)\{Cr(bipy)(C_2O_4)_2\}_4]\cdot 13H_2O$ **17** [32]. Their structure can be viewed as a dimer of trimers. In fact, the lanthanide cations in **17** are bridged by a bis-bidentate oxalato ion which comes from the slow decomposition of the chromium(III) complex (Fig. 17). The values of the intramolecular metal–metal separation are 6.427 [Pr···Pr] and 5.803 Å [average value for Pr···Cr]. Only a few examples of oxalato-bridged 3d–4f complexes are known. The main difficulty in obtaining them, following the building-block approach, arises from the partial decomposition of the anionic tecton with the formation of the insoluble oxalate-containing compounds of formula $Ln_2(C_2O_4)_3\cdot nH_2O$. This process can be slowed down, in order to grow single crystals, by carrying out the diffusion of the reagents through a tetramethoxysilane gel [4d].

Another compound, $[\{Cu(bipy)\}_2(C_2O_4)\{Cr(bipy)(C_2O_4)_2\}_2]\cdot 2H_2O$ **18**, whose structure is shown in Fig. 18, resulted serendipitously by reacting $Ba[Cr(bipy)(C_2O_4)_2]_2\cdot nH_2O$ with $CuSO_4\cdot 5H_2O$ [33]. One oxalato group and the bipyridine molecules coordinated to the copper(II) ion obviously arise from the decomposition of the $[Cr(bipy)(C_2O_4)_2]^-$ precursor. The analysis of its magnetic properties indicate a ferromagnetic coupling between the central copper(II) ions ($J_{CuCu} = +4\,cm^{-1}$) and an antiferromagnetic coupling between Cu(II) and Cr(III) ($J_{CuCr} = -1.3\,cm^{-1}$). The ferromagnetic coupling between the oxalato-bridged copper(II) ions in **18** can be understood having in mind the out-of-plane exchange pathway involved where an equatorial position of one copper(II) ion [O(10) at Cu(1)] is linked to an axial one of the adjacent copper(II) center [Cu1–O10–C25a–O9a–Cu1a; (a) = $-x, -y, -z$]. The copper(II) ions exhibit an elongated octahedral geometry, the magnetic orbital being located in the equatorial plane. For such a situation, where the two equatorial planes of the copper(II) ions are parallel each other and perpendicular to the oxalato plane, the accidental orthogonal-

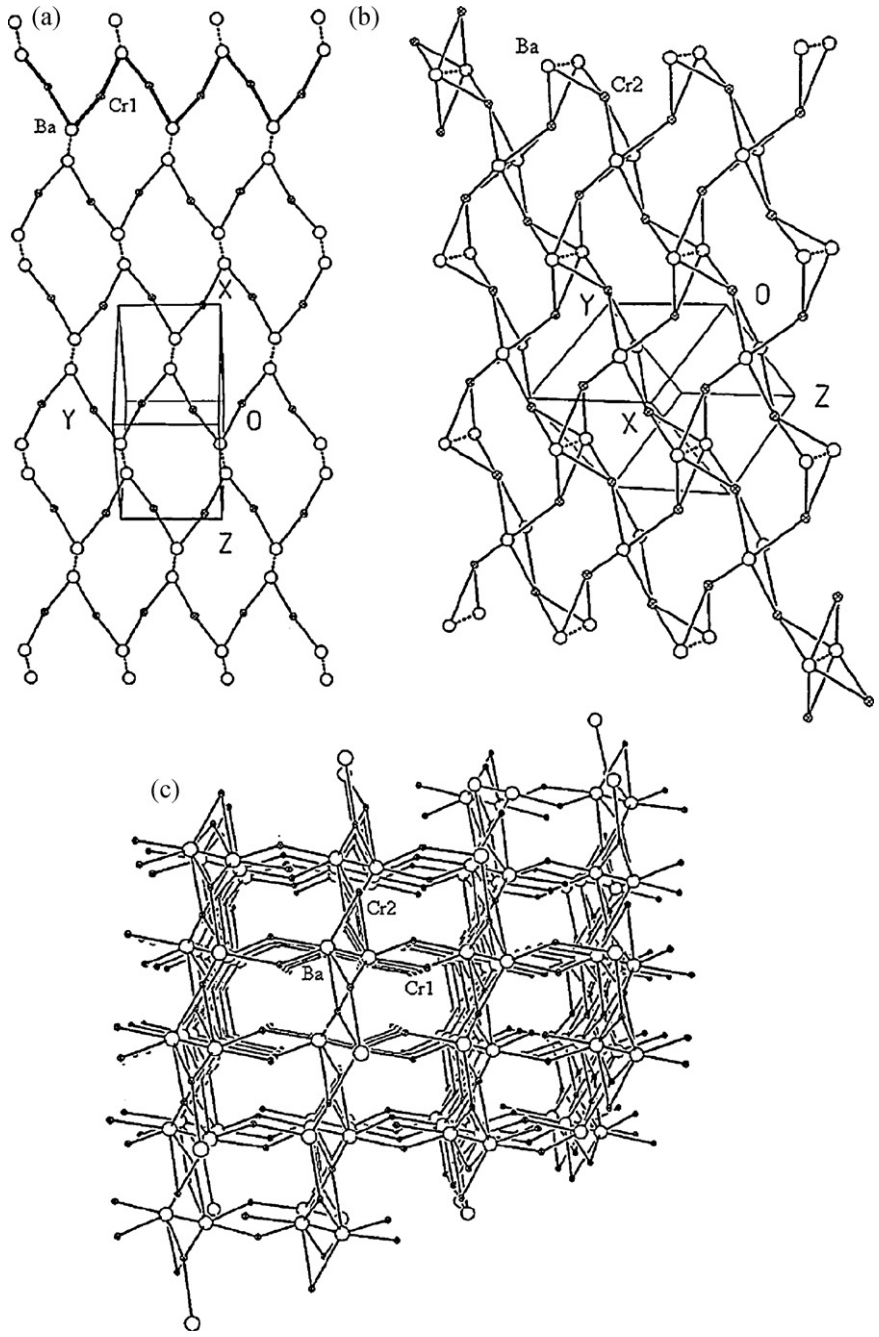

Fig. 24. Construction of the 3D architecture in $[\{Ba(H_2O)\}\{Cr(bipy)(C_2O_4)_2\}_2]\cdot H_2O$ **27.** (a) View of the chickenwire sheet showing the Ba and Cr1 atoms. One chiral helix is in bold style; (b) Connection of the barium ions through Cr2 bridging units; and (c) Perspective view of the scaffolding-like architecture.
Adapted from Ref. [26].

ity is achieved for values of the angle at the apical oxalate-oxygen (β angle in Scheme 7) smaller than 109.5° [34]. As $\beta = 108.7°$ for **18**, a weak ferromagnetic coupling is expected in agreement with the best-fit value.

The release of oxalate ions from $[Cr(AA)(C_2O_4)_2]^-$ was also observed during the reaction between a binuclear [Cu(II)Gd(III)] complex and $K[Cr(bipy)(C_2O_4)_2]$ [35]. One-dimensional $[L^2Cu^{II}Gd^{III}(H_2O)_3(C_2O_4)]^{n+}{}_n$ cationic motifs are formed, whose charge is counterbalanced by the free $[Cr(bipy)(C_2O_4)_2]^-$ anions (H_2L^2 is the Schiff-base obtained by condensation of 3-methoxysalycilaldehyde with 1,3-propanediamine).

Finally, another unexpected situation deals with the release of the chelating ligand. At that respect, during the reaction between $PPh_4[Cr(bpym)(C_2O_4)_2]\cdot H_2O$ and silver(I) perchlorate, the bpym ligand from the precursor is replaced by two water molecules, affording the *cis*-diaquabis(oxalato)chromate(III) species which act as the counterion of the bpym-bridged silver(I) chain $[Ag(bpym)]^{n+}{}_n$ [16]. However, in spite of these examples which evidence a certain lability of the $[Cr(AA)(C_2O_4)_2]^-$ precursor, it behaves as a very stable species in solution and its use as a ligand can be considered as a safe and rational route towards multifunctional heterometallic compounds.

5. Coordination polymers

The formation of coordination polymers is favoured when fully hydrated (solvated) metal ions are used as assembling cations. However, we have seen (Section 4.2) that the assembly process

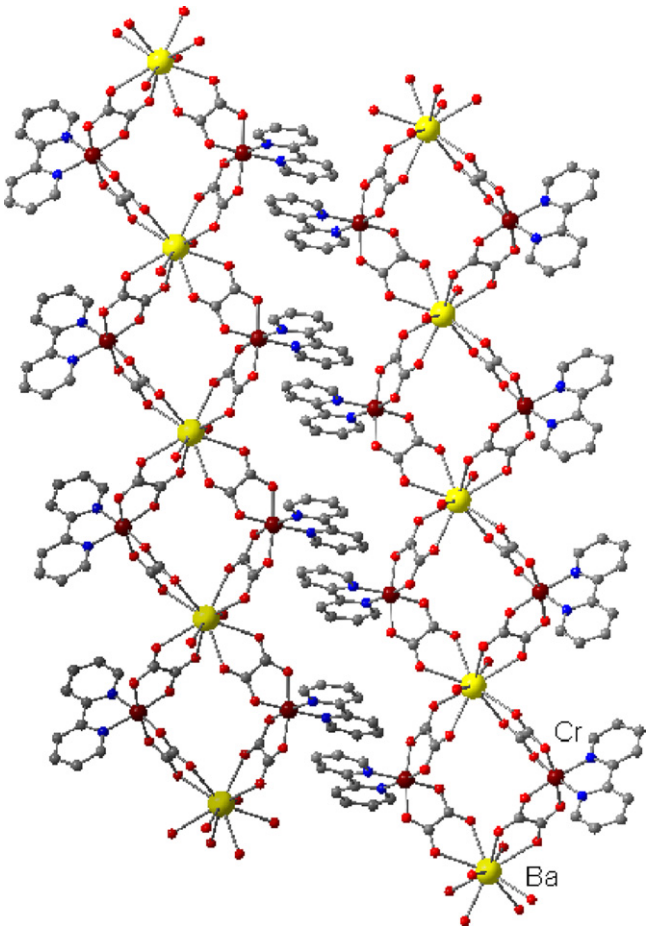

Fig. 25. Packing diagram for compound **28a**, showing the π–π stacking interactions between the bipy ligands from neighboring chains. Adapted from Ref. [39].

between $[M(H_2O)_6]^{2+}$ (M = Cu, Co and Ni) and $[Cr(bipy)(C_2O_4)_2]^-$ ions affords discrete, trinuclear Cr(III)–M(II)–Cr(III) complexes, the central ion being six-coordinated. One way to expand the structure from discrete to coordination polymers is to choose, as assembling cations, metal ions which are able to achieve higher coordination numbers. It is well known that high-spin manganese(II) has no stereochemical preference and it can reach seven- and even eight-coordination. Indeed, a 1D coordination polymer is obtained by reacting $Ba[Cr(bipy)(C_2O_4)_2]_2$ with $MnSO_4$: ${}_1{}^{\infty}[Mn\{Cr(bipy)(C_2O_4)_2\}_2]_n$ **19** [26]. The coordination number of manganese is eight, exhibiting a flattened square antiprism geometry. Each chain is formed of diamond-shaped units sharing the manganese(II) ions, while the two other corners are occupied by the chromium(III) ions (Fig. 19). The values of the Mn···Cr distance vary between 5.533 and 5.573 Å. All the chiral chromium coordinated centers in a chain have the same absolute configuration, either Δ or Λ. Consequently each chain is chiral. Since compound **19** crystallizes in a centrosymmetric space group ($P2_1/c$), chains of opposite chiralities are present in the same crystal.

We have mentioned several times in the preceding sections that many oxalato-bridged heterometallic complexes containing chromium(III) and another transition metal ion were prepared using "$Na[Cr(AA)(C_2O_4)_2]$", "$K[Cr(AA)(C_2O_4)_2]$", or "$Ba[Cr(AA)(C_2O_4)_2]_2$" as starting materials. What about their structures? The crystallographic investigations have shown that these compounds are themselves very interesting coordination polymers.

Let us discuss firstly the systems obtained with univalent assembling cations: Na^+, K^+ and Ag^+. The following four compounds show the same 2D network topology: ${}_2{}^{\infty}[\{Na(H_2O)\}\{Cr(bipy)(C_2O_4)_2\}]\cdot 2H_2O$ **20** [12], ${}_2{}^{\infty}[\{Na(H_2O)\}\{Cr(phen)(C_2O_4)_2\}]\cdot 2H_2O$ **21** [14], ${}_2{}^{\infty}[\{Ag(H_2O)\}\{Cr(dmbipy)(C_2O_4)_2\}]\cdot 3H_2O$ **22** [17], ${}_2{}^{\infty}[\{Na(H_2O)\}\{Cr(pyim)(C_2O_4)_2\}]\cdot 2H_2O$ **23** [pyim = 2-(2′-pyridyl)imidazole] [36]. Their structure is made up of oxalato-bridged Cr(III)–M(I) helical chains, which are linked by centrosymmetric M_2O_2 units (Fig. 20). The Cr_2M_2 moiety is formed through the interaction of one of the oxalato groups with two M atoms simultaneously (Fig. 20a). Each M(I) ion has a coordination number of six. Within each layer, four octanuclear Cr_4M_4 rings and four Cr_2M_2 rhombuses alternate regularly around each Cr_4M_4 unit (Fig. 20b and c). Interestingly, with histamine (hm) as a bidentate co-ligand to chromium, the sodium derivative, ${}_1{}^{\infty}[\{Na(H_2O)\}\{Cr(hm)(C_2O_4)_2\}]\cdot 2H_2O$ **24**, is a 1D coordination polymer, constructed from zigzag Cr(III)–Na(I) chains, connected by centrosymmetric Na_2O_2 units (Fig. 21) [37]. Within each Cr(III)–Na(I) chain, the chromium and sodium coordinated centers have opposite absolute configurations (Δ, Λ), while in the case of the compounds **20**, **21**, **23** each Cr(III)–Na(I) chain is constructed from coordinated chiral metal ions with the same absolute configurations, either (Δ, Δ) or (Λ, Λ).

The reaction between **20** and bis(1-pyrazolyl)methane (bpm) led to a two-dimensional stair-shaped coordination polymer, that results by replacing the aqua ligand from each sodium ion by a bridging bpm ligand, ${}_2{}^{\infty}[\{Na(bpm)\}Cr(bipy)(C_2O_4)_2\}]\cdot 2H_2O$ **25** [38] (Fig. 22).

Only two structures containing univalent potassium as assembling cation were reported. The first one is the compound of formula ${}_2{}^{\infty}[\{K(dmf)\}\{Cr(phen)(C_2O_4)_2\}]\cdot 0.5H_2O$ **26** [18]. Although here

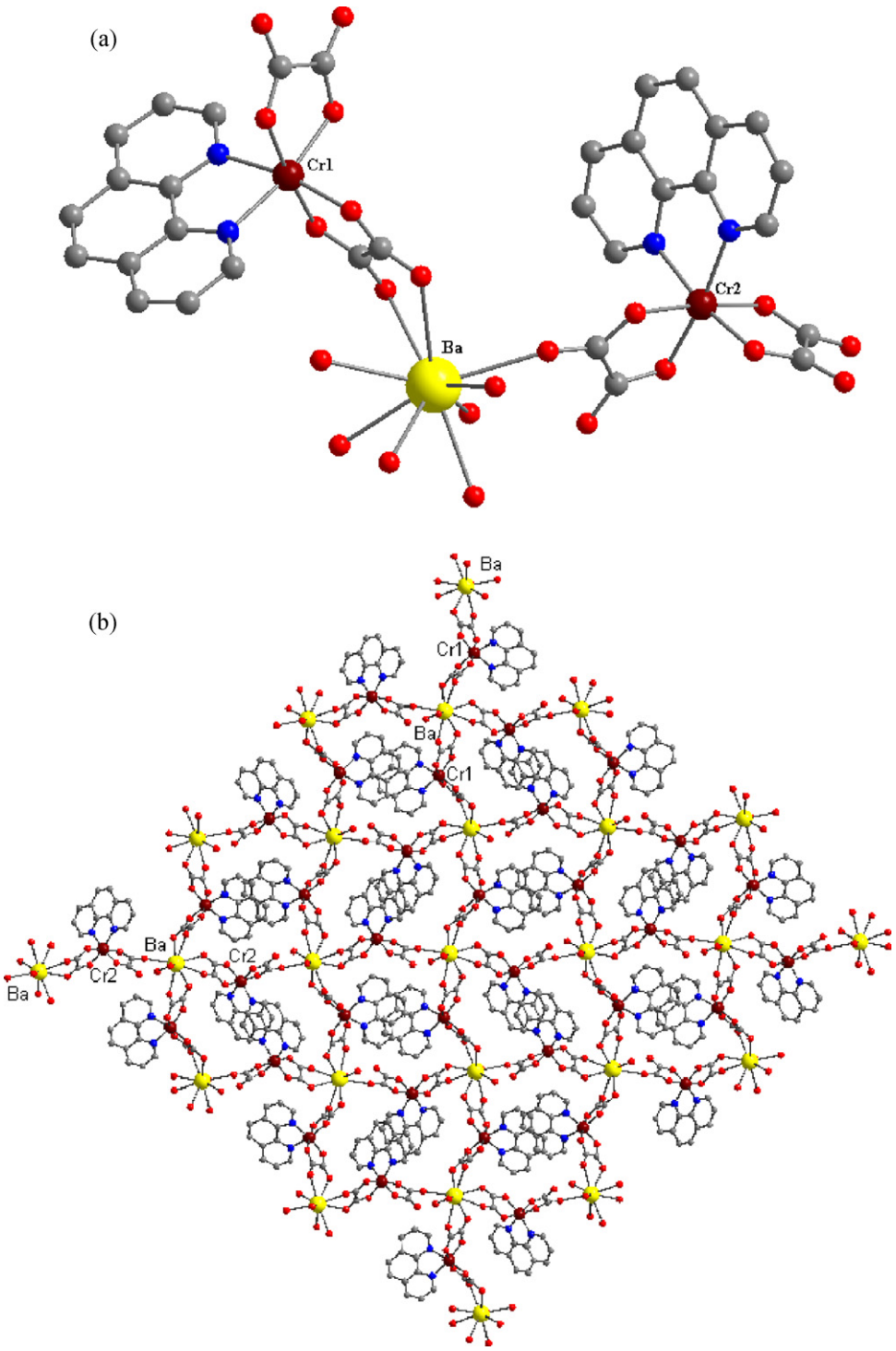

Fig. 26. Construction of a 2D layer in compound **30**. (a) The independent heterotrinuclear enitity; and (b) perspective view of a 2D coordination polymer, showing the stacking intercations between the ligands.
Adapted from Ref. [39].

again the M^+ ions are six-coordinated, like in the complexes **21**–**23**, the connectivity mode is different: two potassium cations are linked by four oxalato groups arising from four $\{Cr(phen)(C_2O_4)_2\}$ building blocks (Fig. 23a), resulting in a kind of "pillar". Two out of these four units act as terminal ligands, that is, the second oxalato group from each one is not coordinated to another potassium cation. The shortest distance between the potassium ions is 3.939 Å. The four K···Cr units form a four-tipped star around the K···K pillars. Infinite thick layers are thus formed (Fig. 23b).

A very interesting case is the one of barium(II) as an assembling cation. The recrystallization from water of the crude products obtained following the Broomhead's procedure (Scheme 2) afforded two types of compounds, for both bipy and phen series:

$[\{Ba(H_2O)\}\{Cr(bipy)(C_2O_4)_2\}_2]\cdot H_2O$ **27** [26]; $[\{Ba(H_2O)_2\}\{Cr(bipy)(C_2O_4)_2\}_2]\cdot 4H_2O$ **28a** [39], $[\{Ba(H_2O)_2\}\{Cr(dmbipy)(C_2O_4)_2\}_2]\cdot 8.5H_2O$ **28b** [17]; $[\{Ba(H_2O)_2\}\{Cr(phen)(C_2O_4)_2\}_2]\cdot 4H_2O$ **29** [40,41]; $[\{Ba(H_2O)_2\}\{Cr(phen)(C_2O_4)_2\}_2]$ **30** [39].

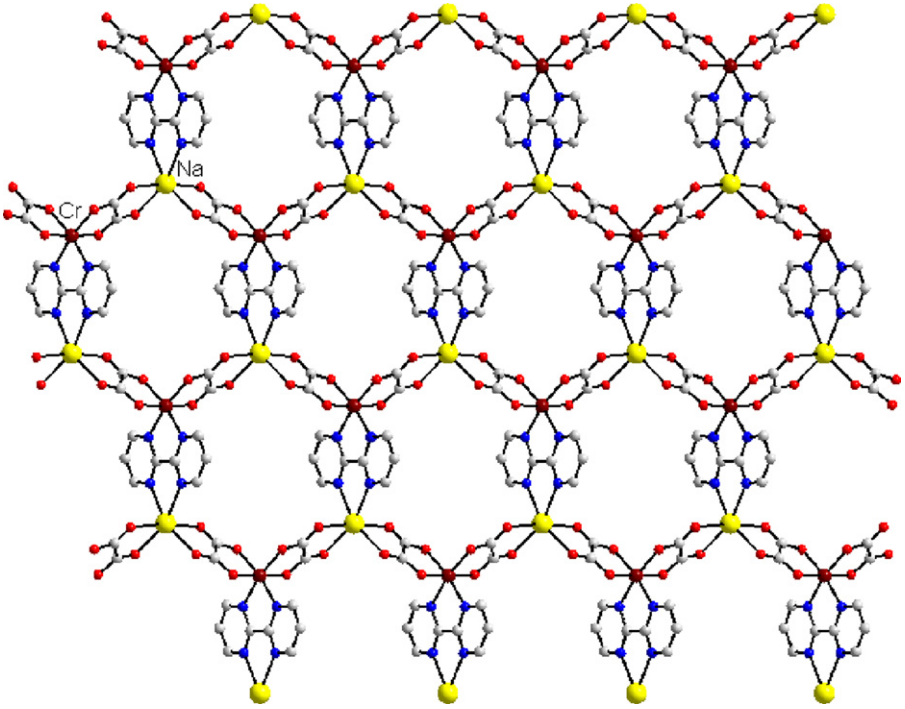

Fig. 27. View of the structure of $_2{}^{\infty}$[NaCr(bpym)$(C_2O_4)_2$]·5H_2O **32**.

Adapted from Ref. [42].

Compound **27** is a 3D coordination polymer. The complexity of its structure arises from three bridging modes of the oxalato groups (Scheme 8): the two oxalato groups bound to Cr1 exhibit two bridging modes, while those coordinated to Cr2 are involved in only one type of bridging. The barium cations are ten-coordinated (nine oxalato oxygen atoms and one aqua ligand). Pairs of barium cations form a pillar, similar to the one constructed by two potassium cations in **26**. The Ba···Ba distance is quite short (4.138 Å). Each barium cation is connected to two Cr1 units almost in the same plane forming a chickenwire sheet (Fig. 24a). The Cr2 units connecting the barium cations form a helix, running along the crystallographic *b*-axis. The sheets are linked together through the barium pillars, where two barium atoms forming a pillar are connected by four oxalato groups arising from Cr2 units (Fig. 24b). The four bridging Cr2 units form an elongated four-tipped star around the Ba···Ba pillar approximately perpendicular to the Ba···Cr1 sheets, resulting in an infinite 3D architecture (Fig. 24c). The crystal structure of **28a** is completely different. It consists of neutral chains, with diamond-shaped units sharing the barium atoms, while the two other corners are occupied by chromium atoms. The barium cations are connected through $[Cr(bipy)(C_2O_4)_2]^-$ ions, with the oxalato groups exhibiting the classical bis-bidentate bridging mode. The coordination number of barium is ten: eight oxygen atoms from the four oxalato bridges and two aqua ligands. The shortest intrachain metal–metal separations are: Ba···Cr = 6.121, Cr···Cr = 12.24, Ba···Ba = 9.511 Å. The neighboring chains interact through π–π contacts established between the bipy ligands (3.6 Å) (Fig. 25).

Compound **29** exhibits the same topology as complexes **28a** and **28b**. Compounds **29** and **30** differ only through the number of crystallization water molecules. However, their network

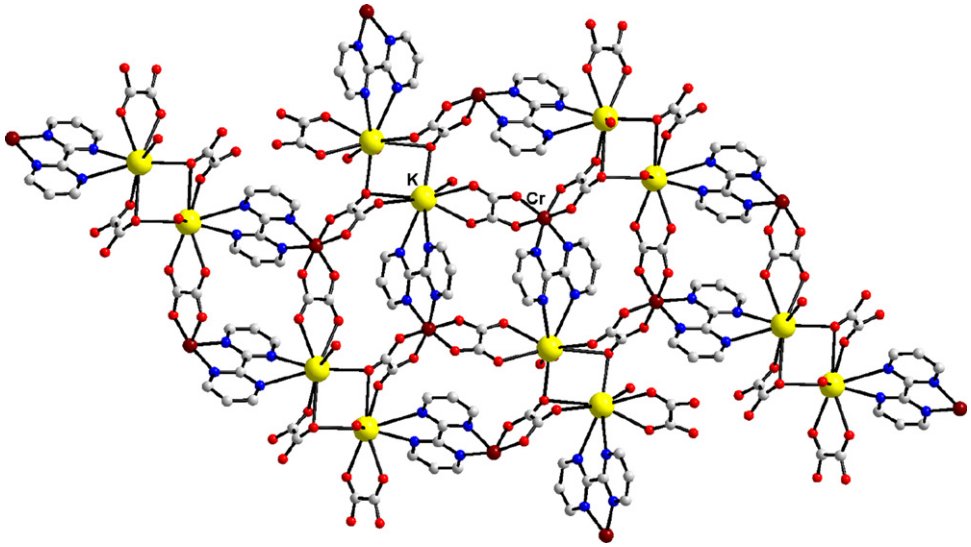

Fig. 28. View of the 2D structure of $_2{}^{\infty}$[{K(H_2O)}Cr(bpym$(C_2O_4)_2$] **33**.

Adapted from Ref. [43].

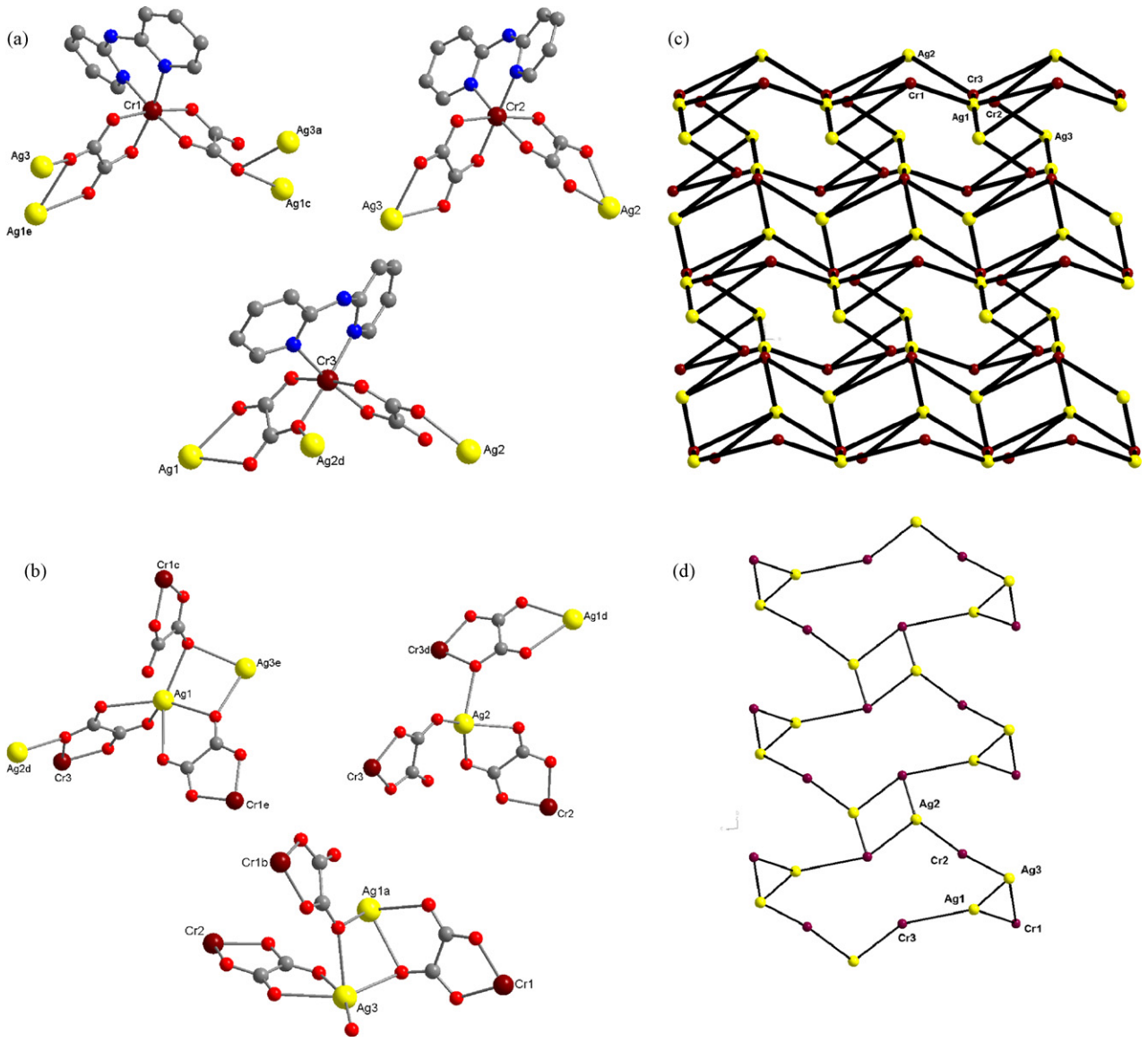

Fig. 29. Construction of the 2D layers in $_2^{\infty}[\{Ag_3(H_2O)\}\{Cr(dpa)(C_2O_4)_2\}_3]\cdot 2H_2O$ **34**; (a) views of the three crystallographically independent chromium atoms; (b) views of the crystallographically independent silver atoms; (c) view of a layer along the crystallographic *c* axis; and (d) view of a layer along the ceystallographic *a*-axis. Adapted from Ref. [44].

topologies are completely different. While **29** is a 1D coordination polymer, the structure of **30** consists of a 2D framework, which is made up of crystallographically independent heterotrinuclear entities of formula $[Ba(H_2O)_2\{Cr(phen)(C_2O_4)_2\}_2]$, with two different chromium atoms, Cr1 and Cr2 (Fig. 26a). The structure can be described as follows: the barium ions are connected through $[Cr(1)(phen)(C_2O_4)_2]^-$ ions, with both oxalato groups acting as bis-bidentate ligands, resulting in zigzag chains. These chains are then interconnected by $[Cr(2)(phen)(C_2O_4)_2]^-$ ions, from which one oxalato group acts as a bis-bidentate ligand, while the second one acts as a bidentate ligand towards chromium and as a monodentate ligand towards barium. A two-dimensional network results, with irregular octagonal meshes, which are filled by stacked phenanthroline ligands belonging to two adjacent chromium units (Fig. 26b). The separation between the two phen planes is *ca.* 3.3 Å. The barium atoms nine-coordinated: seven oxalato oxygen atoms and two aqua ligands. The intermetallic distances within a mesh are: Ba1–Cr1 = 5.985; 6.033 Å; Ba1–Cr2 = 5.980; 6.616 Å. The longest distance corresponds to the metal ions bridged by the bidentate–monodentate oxalato group.

The examples discussed above show that the number of the coordinated and crystallization water molecules is crucial for the dimensionality of the oxalato-bridged Ba(II)–Cr(III) frameworks. In the case of the oxalato-bridged Ba(II)–Cr(III)-bipy system, the highest dimensionality (3D) is observed with compound **27**, with one aqua ligand to barium. If the number of aqua ligands coordinated to barium increases to two, then a one-dimensional coordination polymer is obtained: $_1^{\infty}[BaCr_2(bipy)_2(C_2O_4)_4(H_2O)_2]\cdot 4H_2O$ **28a** whose structure is similar to the one of the phenanthroline derivative, $_1^{\infty}[BaCr_2(phen)_2(C_2O_4)_4(H_2O)_2]\cdot 4H_2O$ **29**, with the same number of water molecules. Within the dmbipy series, the barium complex, $[\{Ba(H_2O)_2\}\{Cr(dmbipy)(C_2O_4)_2\}_2]\cdot 8.5H_2O$ **28b**, shows also a 1D structure [17]. Compound **30**, $_2^{\infty}[BaCr_2(phen)_2(C_2O_4)_4(H_2O)_2]$, with only two water molecules, both of them coordinated to the barium atom, exhibits a 2D structure. We mention also a strontium(II) derivative, $[Sr\{Cr(dpa)(C_2O_4)_2\}_2]\cdot 8H_2O$ **31**, whose structure is similar to **19**, the strontium cations being eight-coordinated [15].

Interesting network topologies are expected when not only the oxalato groups but also the chelating diimine coordinated to the chromium(III) can itself act as a bridge. Such a ligand is 2,2′-bipyrimidine. Two 2D structures constructed from $[Cr(bpym)(C_2O_4)_2]^-$ tectons and alkali metal assembling cations have been reported: $_2^\infty[NaCr(bpym)(C_2O_4)_2]\cdot 5H_2O$ **32** [42], and $_2^\infty[\{K(H_2O)\}Cr(bpym(C_2O_4)_2]$ **33** [43].

The structure of **32** is made up of parallel sheets each one consisting of infinite hexagonal array of chromium(III) and sodium(I) cations bridged by bis-bidentate oxalato and bpym ligands (Fig. 27).

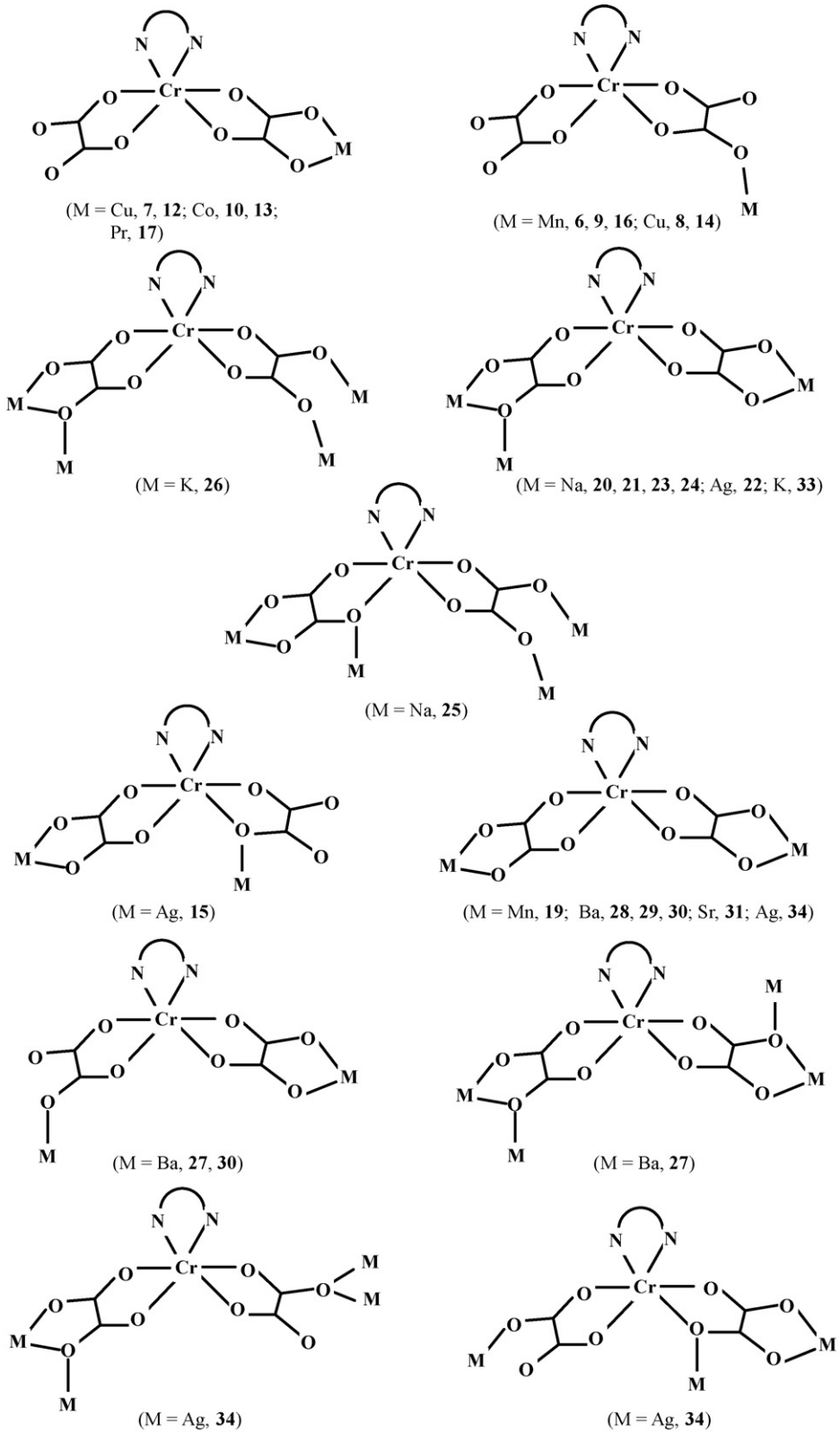

Scheme 9.

A cyclic pentameric water aggregate is hosted in each hexagonal hole of the sheets.

The potassium derivative, **33**, is also a 2D coordination polymer but the connectivity modes involving the oxalato bridges are different (Fig. 28). One oxalato group and the bpym molecule act as bis-chelating ligands towards chromium(III) and potassium(I). The other oxalato group exhibits a very rare bridging mode connecting one chromium ion to two potassium ions. The potassium ions are eight-coordinated. The shortest intermetallic distances are Cr···Cr = 6.974 and K···K = 3.841 Å.

Finally, we mention a coordination polymer that has been assembled from the reaction of $[Cr(dpa)(C_2O_4)_2]^-$ with Ag^+ in aqueous solution: ${}_2{}^{\infty}[\{Ag_3(H_2O)\}\{Cr(dpa)(C_2O_4)_2\}_3]\cdot 2H_2O$ **34** [44]. The structure is quite complicated, and it consists of thick layers constructed from three crystallographically independent chromium (Cr1, Cr2, Cr3) and silver (Ag1, Ag2, Ag3) metal ions. Each $[Cr(dpa)(C_2O_4)_2]^-$ unit acts a ligand towards the silver atoms. The corresponding six oxalato groups exhibit five different bridging modes (Fig. 29a). Ag1 and Ag3 are five-coordinated, with distorted square-pyramidal geometries, while Ag2 is four-coordinated, with a distorted tetrahedral stereochemistry (Fig. 29b). Decagon nonplanar and centrosymmetric bimetallic rhombuses are formed from the arrangement of the $[Cr(dpa)(C_2O_4)_2]^-$ and Ag^+ ions (Fig. 29c). Each metallocycle is linked to other four ones through two Ag_2Cr_2 rhombuses along the *b*-axis (involving Cr3 and Ag2 atoms) and across $[Cr(dpa)(C_2O_4)_2]^-$ pillars along the *a*-axis, leading to a layer growing in the *ab*-plane.

6. Conclusions

The cases discussed above illustrate the exceptional synthetic potential of the $[Cr(AA)(C_2O_4)_2]^-$ ions to act as tectons in constructing heterometallic complexes. The variety of the resulting structures is mainly due to the stereochemical preferences of the assembling cations, as well as to the versatile coordination behaviour of the oxalato ligand, that is, the wide range of coordination modes it can adopt. Scheme 9 illustrates all the different functions of the $[Cr(AA)(C_2O_4)_2]^-$ metalloligands that have been identified so far. The nuclearity/dimensionality and the topology of the resulting clusters/coordination polymers are also influenced by auxiliary co-ligands attached to the assembling cation and by additional bridges. The aromatic diimines and the oxalato ligands coordinated to chromium can be involved in supramolecular interactions as well, which control the packing of the molecules in the crystal. The aromatic diimines from two $\{Cr(AA)(C_2O_4)_2\}$ moieties have a strong tendency to associate through π–π contacts. When uncoordinated to a second metal ion, the $[Cr(AA)(C_2O_4)_2]^-$ ions form supramolecular dimers. The way in which the aromatic rings overlap influences the nature of the exchange interaction (ferro- or antiferromagnetic) within the supramolecular dimers. As far as the oxalato ligand is concerned, apart its ability to interact with another metal ion, it can also act as a hydrogen bond acceptor [13,25,39,45].

The use of the mixed-ligand bis-oxalato tectons in crystal engineering, in order to obtain porous materials, remains largely unexploited. Only recently the cobalt(III) analogue, $[Co(en)(C_2O_4)_2]^-$, was shown to generate 3D coordination networks with remarkable gas storage properties [46]. The construction of chiral crystals, starting from only one of the $[M(AA)(C_2O_4)_2]^-$ enantiomers, is also an appealing and challenging research topic.

Acknowledgements

Financial support from the CNCSIS (Romania), Grant IDEI-1912/2009, Ministerio Español de Ciencia e Innovación (MECI, Spain) (Project CTQ2007-61690 and Consolider-Ingenio in Molecular Nanoscience, CSD2007-00010), and the Generalitat Valenciana (GV, Spain) (PROMETEO2009/108) is gratefully acknowledged. Special thanks are due to all our co-workers, colleagues and students whose names appear in the references listed. Without them, this work would not be. One of us (M. A.) is grateful to the University Valencia for a visiting professorship funding in 2010.

References

[1] O. Kahn, Molecular Magnetism, Wiley-VCH, New York, 1993, and references therein.
[2] M. Verdaguer, M. Julve, A. Michalowicz, O. Kahn, Inorg. Chem. 22 (1983) 2624.
[3] See, for example:
(a) F. Lloret, M. Julve, M. Mollar, I. Castro, J. Latorre, J. Faus, J. Chem. Soc. Dalton Trans. (1989) 729;
(b) M. Ohba, H. Tamaki, N. Matsumoto, H. Okawa, S. Kida, Chem. Lett. (1991) 1157;
(c) M. Ohba, H. Tamaki, N. Matsumoto, H. Okawa, Inorg. Chem. 32 (1993) 5385;
(d) T. Sanada, T. Suzuki, T. Yoshida, S. Kaizaki, Inorg. Chem. 37 (1998) 4712;
(e) M.A. Subhan, H. Nakata, T. Suzzuki, J.-H. Choi, S. Kaizaki, J. Lumin. 101 (2003) 307.
[4] See, for example:
(a) Y. Pei, Y. Journaux, O. Kahn, Inorg. Chem. 28 (1989) 100;
(b) O. Kahn, Adv. Inorg. Chem. 43 (1995) 179;
(c) O. Costisor, K. Mereiter, M. Julve, F. Lloret, Y. Journaux, W. Linert, M. Andruh, Inorg. Chim. Acta 324 (2001) 352;
(d) S. Decurtins, R. Pellaux, G. Antorrena, F. Palacio, Coord. Chem. Rev. 190–192 (1999) 841;
(e) M. Pilkington, S. Decurtins, J.S. in, M. Miller, Drillon (Eds.), Magnetism: Molecules to Materials II, VCH, Weinheim, 2001, p. 339;
(f) R. Clément, S. Decurtins, M. Gruselle, C. Train, in: W. Linert, M. Verdaguer (Eds.), Molecular Magnets. Recent Highlights, Springer, Wien, 2003, p. 1;
(g) M. Pilkington, S. Decurtins in, J.A. McCleverty, T.J. Meyer (Eds.), Comprehensive Coordination Chemistry II, vol. 7, Elsevier, Amsterdam, 2004, p. 177;
(h) M. Gruselle, C. Train, K. Boubekeur, P. Gredin, N. Ovanesyan, Coord. Chem. Rev. 250 (2006) 2491;
(i) H. Amouri, M. Gruselle, Chirality in Transition Metal Chemistry, Wiley, Chichester, 2008.
[5] See, for example:
(a) H. Tamaki, Z.J. Zhong, N. Matsumoto, S. Kida, M. Koikawa, N. Achiwa, Y. Hashimoto, H. Okawa, J. Am. Chem. Soc. 114 (1992) 6974;
(b) L.O. Atovmyan, G.V. Shilov, R.N. Lyobovsaya, E.L. Zhilyaeva, N.S. Ovanesyan, S.I. Pirumova, I.G. Gusakovskaya, Y.K. Morozov, JETP Lett. 58 (1993) 766;
(c) S. Decurtins, H.W. Schmalle, H.R. Oswald, A. Linden, J. Ensling, P. Gütlich, A. Hauser, Inorg. Chim. Acta 216 (1994) 65;
(d) L.P. Farrell, T.W. Hambley, P.A. Lay, Inorg. Chem. 34 (1995) 757;
(e) R. Pellaux, H.W. Schmalle, R. Huber, P. Fischer, T. Hauss, B. Ouladdiaf, S. Decurtins, Inorg. Chem. 36 (1997) 2301;
(f) S. Decurtins, M. Gross, H.W. Schmalle, S. Ferlay, Inorg. Chem. 37 (1998) 2443;
(g) R. Andrés, M. Gruselle, B. Malézieux, M. Verdaguer, J. Vaissermann, Inorg. Chem. 38 (1999) 4637;
(h) E. Coronado, J.R. Galán-Mascarós, C.J. Gómez-García, J. Ensling, P. Gütlich, Chem. Eur. J. 6 (2000) 552;
(i) E. Coronado, J.R. Galán-Mascarós, C.J. Gómez-García, V. Laukhin, Nature 408 (2000) 447;
(j) M. Gruselle, R. Thouvenot, B. Malézieux, C. Train, P. Gredin, T.V. Demeschik, L.L. Troitskaya, V.I. Sokolov, Chem. Eur. J. 10 (2004) 4763;
(k) M. Clemente-León, E. Coronado, J.C. Dias, A. Soriano-Portillo, R.D. Willett, Inorg. Chem. 47 (2008) 6458;
(l) C. Train, R. Gheorghe, V. Krstic, L.M. Chamoreau, N.S. Ovanesyan, A.J.L.G. Rikken, M. Gruselle, M. Verdaguer, Nat. Mater. 7 (2008) 729.
[6] (a) M. Clemente-León, E. Coronado, M. López-Jordá, G. Mínguez-Espllargas, A. Soriano-Portillo, J.C. Waerenborgh, Chem. Eur. J. 16 (2010) 2207;
(b) M. Clemente-León, E. Coronado, M. López-Jordá, Dalton Trans. 39 (2010) 4903.
[7] (a) S. Bénard, P. Yu, J.P. Audière, E. Rivière, R. Clément, J. Guilhem, L. Tchertanov, K. Nakatani, J. Am. Chem. Soc. 122 (2000) 9444;
(b) C. Train, T. Nuida, R. Gheorghe, M. Gruselle, S.I. Ohkoshi, J. Am. Chem. Soc. 131 (2009) 16838.
[8] H. Okawa, A. Shigematsu, M. Sadakiyo, T. Miyagawa, K. Yoneda, M. Ohba, H. Kitagawa, J. Am. Chem. Soc. 131 (2009) 13516.
[9] (a) S. Decurtins, H.W. Schmalle, P. Schneuwly, H.R. Oswald, Inorg. Chem. 32 (1993) 1888;
(b) S. Decurtins, H.W. Schmalle, P. Schneuwly, J. Ensling, P. Gütlich, J. Am. Chem. Soc. 116 (1994) 9521;
(c) S. Decurtins, H.W. Schmalle, R. Pellaux, P. Schnewly, A. Hauser, Inorg. Chem. 35 (1996) 1451;
(d) P. Román, C. Guzmán-Miralles, A. Luque, Dalton Trans. (1996) 3985;
(e) M. Hernández-Molina, F. Lloret, C. Ruiz-Pérez, M. Julve, Inorg. Chem. 37 (1998) 4131;
(f) R. Sieber, S. Decurtins, H. Stoeckli-Evans, C. Wilson, D. Yufit, J.A.K. Howard, S.C. Capelli, A. Hauser, Chem. Eur. J. 6 (2000) 361;
(g) R. Andrés, M. Brissard, M. Gruselle, C. Train, J. Vaissermann, B. Malézieux,

J.P. Jamet, M. Verdaguer, Inorg. Chem. 40 (2001) 4633;
(h) E. Coronado, J.R. Galán-Mascarós, C.J. Gómez-García, E. Martínez-Ferrero, M. Almeida, J.C. Waerenborgh, Eur. J. Inorg. Chem. (2005) 2064.
[10] I. Imaz, G. Bravic, J.-P. Sutter, Dalton Trans. (2005) 2691.
[11] J.A. Broomhead, Aust. J. Chem. 15 (1962) 228.
[12] M.C. Muñoz, M. Julve, F. Lloret, J. Faus, M. Andruh, J. Chem. Soc. Dalton Trans. (1998) 3125.
[13] R. Lescouëzec, G. Marinescu, J. Vaissermann, F. Lloret, J. Faus, M. Andruh, M. Julve, Inorg. Chim. Acta 350 (2003) 131.
[14] G. Marinescu, M. Andruh, R. Lescouëzec, M.C. Muñoz, J. Cano, F. Lloret, M. Julve, New J. Chem. 24 (2000) 527.
[15] R. Lescouëzec, G. Marinescu, M.C. Muñoz, D. Luneau, M. Andruh, F. Lloret, J. Faus, M. Julve, J.A. Mata, R. Llusar, J. Cano, New J. Chem. 25 (2001) 1224.
[16] G. Marinescu, R. Lescouëzec, D. Armentano, G. De Munno, M. Andruh, S. Uriel, R. Llusar, F. Lloret, M. Julve, Inorg. Chim. Acta 336 (2002) 46.
[17] M. Viciano-Chumillas, N. Marino, I. Sorribes, C. Vicent, F. Lloret, M. Julve, CrystEngComm 10 (2010) 122.
[18] F.D. Rochon, G. Massarweh, Can. J. Chem. 77 (1999) 2059.
[19] A.M. Madalan, E. Canadell, P. Aubane-Senzier, D. Branzea, N. Avarvari, M. Andruh, New J. Chem. 32 (2008) 333.
[20] (a) M. Clemente-Léon, E. Coronado, M.C. Giménez-López, F.M. Romero, Inorg. Chem. 46 (2007) 11266;
(b) M.C. Giménez-López, M. Clemente-Léon, E. Coronado, F.M. Romero, S. Shova, J.-P. Tuchagues, Eur. J. Inorg. Chem. (2005) 2783.
[21] V. Russell, D. Craig, M. Scudder, I. Dance, CrystEngComm 3 (2001) 96.
[22] (a) M. Wesolek, D. Meyer, J.A. Osborn, A. De Cian, J. Fischer, A. Derory, P. Legoll, M. Drillon, Angew. Chem. Int. Ed. Engl. 33 (1994) 1592;
(b) A.J. Amoroso, J.C. Jeffery, P.L. Jones, J.A. McCleverty, P. Thornton, M. Ward, Angew. Chem. Int. Ed. Engl. 34 (1995) 1443.
[23] H.M. McConnell, J. Chem. Phys. 39 (1963) 1910.
[24] S. Nastase, F. Tuna, C. Maxim, C.A. Muryn, N. Avarvari, R.E.P. Winpenny, M. Andruh, Cryst. Growth Des. 7 (2007) 1825.
[25] G. Marinescu, D. Visinescu, A. Cucos, M. Andruh, Y. Journaux, V. Kravtsov, Yu.A. Simonov, J. Lipkowski, Eur. J. Inorg. Chem. (2004) 2914.
[26] F.D. Rochon, R. Melanson, M. Andruh, Inorg. Chem. 35 (1996) 6086.
[27] N. Stanica, C.V. Stager, M. Cimpoesu, M. Andruh, Polyhedron 17 (1998) 1787.
[28] M. Andruh, R. Melanson, C.V. Stager, F.D. Rochon, Inorg. Chim. Acta 251 (1996) 309.
[29] J. Vallejo, I. Castro, L. Cañadillas-Delgado, C. Ruiz-Pérez, J. Fernando-Soria, R. Ruiz-García, J. Cano, F. Lloret, M. Julve, Dalton Trans. 39 (2010) 2350.
[30] D. Visinescu, J.P. Sutter, C. Ruiz-Pérez, M. Andruh, Inorg. Chim. Acta 359 (2006) 433.
[31] (a) S. Ménage, S.E. Vítols, P. Bergerat, E. Codjovi, O. Kahn, J.J. Girerd, M. Guillot, X. Solans, T. Calvet, Inorg. Chem. 30 (1991) 2666;
(b) M. Verdaguer, PhD Thesis, University of Orsay, France, 1984;
(c) J. Glerup, P.A. Goodson, D.J. Hodgson, K. Michelsen, Inorg. Chem. 34 (1995) 6255;
(d) W.-Y. Wu, Y. Song, Y.-Z. Li, X.-Z. You, Inorg. Chem. Commun. 8 (2005) 732.
[32] X. Zhang, Y. Cui, F. Zheng, J. Huang, Chem. Lett. (1999) 1111.
[33] E. Coronado, M.C. Giménez, C.J. Gómez-García, F.M. Romero, Polyhedron 22 (2003) 3115.
[34] D. Cangussu, H.O. Stumpf, H. Adams, J.A. Thomas, F. Lloret, M. Julve, Inorg. Chim. Acta 358 (2005) 2292, and references therein.
[35] R. Gheorghe, P. Cucos, M. Andruh, J.-P. Costes, B. Donnadieu, S. Shova, Chem. Eur. J. 12 (2006) 187.
[36] L. Zhang, Y.-Y. Ge, F. Peng, M. Du, Inorg. Chem. Commun. 9 (2006) 486.
[37] N. Sakagami, E. Kita, P. Kita, J. Wisniewska, S. Kaizaki, Polyhedron 18 (1999) 2001.
[38] L. Zhang, P. Cheng, L.-F. Tang, L.-H. Weng, Z.-H. Jiang, D.-Z. Liao, S.-P. Yan, G.-L. Wang, Chem. Commun. (2000) 717.
[39] G. Marinescu, M. Andruh, M. Julve, F. Lloret, R. Llusar, S. Uriel, J. Vaissermann, Cryst. Growth Des. 5 (2005) 261.
[40] M. Andruh, in: G. Ondrejovic, A. Sirota (Eds.), Coordination Chemistry at the Turn of the Century, STU Press, Bratislava, 1999, p. 31.
[41] K. Larsson, Acta Cryst. E 57 (2001) 195.
[42] G. De Munno, D. Armentano, M. Julve, F. Lloret, R. Lescouëzec, J. Faus, Inorg. Chem. 38 (1999) 2234.
[43] F. Bérézovsky, A.A. Hajem, S. Triki, J. Sala Pala, P. Molinié, Inorg. Chim. Acta 284 (1999) 8.
[44] C. Yuste Vivas, F.S. Delgado, C. Ruiz-Pérez, M. Julve, CrystEngComm 6 (2004) 11.
[45] (a) S. Bruda, M. Andruh, H.W. Roesky, Y. Journaux, M. Noltemeyer, E. Rivière, Inorg. Chem. Commun. 4 (2001) 111;
(b) C. Paraschiv, S. Ferlay, M.W. Hosseini, N. Kyritsakas, J.-M. Planeix, M. Andruh, Rev. Roum. Chim. 52 (2007) 101;
(c) D. Visinescu, J.-P. Sutter, H.W. Roesky, J. Magull, M. Andruh, Rev. Roum. Chim. 50 (2005) 737.
[46] (a) C. Borel, M. Håkansson, L. Öhrström, CrystEngComm 8 (2006) 666;
(b) C. Borel, K. Davies, P. Handa, G. Hedberg, C.L. Olivier, S.A. Bourne, M. Håkansson, V. Langer, L. Öhrström, Cryst. Growth Des. 10 (2010) 1971.